AD-A113 128 MATERIALS SCIENCES CORP SPRING HOUSE PA F/G 11/4
ELEVATED TEMPERATURE BEHAVIOR OF METAL-MATRIX COMPOSITES.(U)
NOV 81 Z HASHIN, E A HUMPHREYS F49620-79-C-0059
UNCLASSIFIED MSC/TFR/1214/1502 AFOSR-TR-82-0212 NL

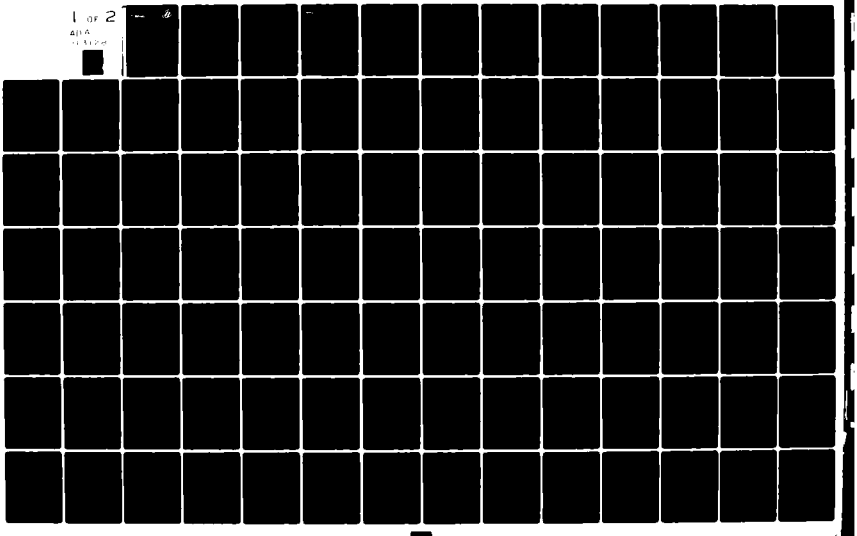

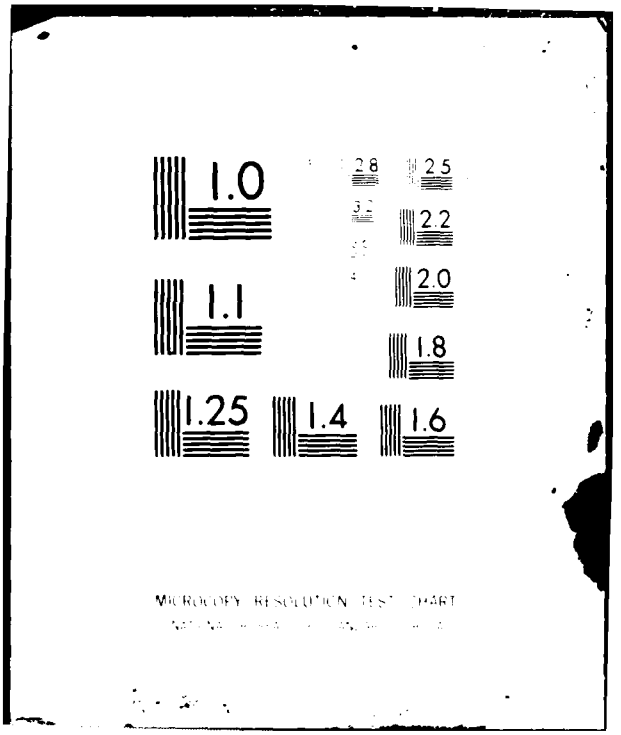
1.0
1.1
1.25
1.4
1.6
2.0
2.2
MICROCOPY RESOLUTION TEST CHART

Materials Sciences Corporation

ELEVATED TEMPERATURE BEHAVIOR OF METAL-MATRIX COMPOSITES

ZVI HASHIN AND E. A. HUMPHREYS

The views and conclusions contained in this document are those of the authors and should not be interpreted as necessarily representing the official policies or endorsements, either expressed or implied, of the Air Force Office of Scientific Research of the U.S. Government.

Air Force Office of Scientific Research
Bolling Air Force Base, D.C.

MSC TFR 1214/1502
November, 1981

F49620-79-C-0059

Unclassified

SECURITY CLASSIFICATION OF THIS PAGE (When Data Entered)

REPORT DOCUMENTATION PAGE	READ INSTRUCTIONS BEFORE COMPLETING FORM
AFOSR-TR- 82-0212 ACCESSION NO	3 RECIPIENT'S CATALOG NUMBER
4. TITLE (and Subtitle) "ELEVATED TEMPERATURE BEHAVIOR OF METAL-MATRIX COMPOSITES"	5 TYPE OF REPORT & PERIOD COVERED Final Report 4/1/79 to 9/30/81 6 PERFORMING ORG REPORT NUMBER
7. AUTHOR(s) Zvi Hashin E. A. Humphreys	8. CONTRACT OR GRANT NUMBER(s) F49620-79-C-0059
9 PERFORMING ORGANIZATION NAME AND ADDRESS Materials Sciences Corporation Gwynedd Plaza II Bethlehem Pike Spring House, PA 19477	10. PROGRAM ELEMENT PROJECT TASK AREA & WORK UNIT NUMBERS 61102F 2307/B1
11. CONTROLLING OFFICE NAME AND ADDRESS Air Force Office of Scientific Research/NA Bolling AFB, DC 20332	12. REPORT DATE November, 1981 13 NUMBER OF PAGES 108
14. MONITORING AGENCY NAME & ADDRESS(if different from Controlling Office)	15. SECURITY CLASS (of this report) Unclassified 15a DECLASSIFICATION DOWNGRADING SCHEDULE

16. DISTRIBUTION STATEMENT (of this Report)

Approved for public release, distribution unlimited

17. DISTRIBUTION STATEMENT (of the abstract entered in Block 20, if different from Report)

18. SUPPLEMENTARY NOTES

19. KEY WORDS (Continue on reverse side if necessary and identify by block number)

Metal Matrix Composites
Graphite Fibers
Plasticity
Temperature Dependence
Plasticity Theory
Numerical Analysis

20. ABSTRACT (Continue on reverse side if necessary and identify by block number)

A three fold approach is utilized to develop three-dimensional temperature dependent plasticity relations for unidirectional metal-matrix composites. First, two elasto-plastic boundary value problems are formulated for a typical repeating element in a hexagonal array of fibers. This is used to numerically determine temperature dependent stress-strain relations for loadings such as transverse tension, transverse shear, and axial shear. Next, global plasticity considerations are used to construct isothermal, incremental stress-strain relations for a transversely isotropic fiber composite in terms of the

DD FORM 1 JAN 73 1473

UNCLASSIFIED

SECURITY CLASSIFICATION OF THIS PAGE (When Data Entered)

20. (continued)

known one-dimensional stress-strain relations. Finally, these results are extended to include changes in temperature resulting in a set of effective stress-strain relations incremental in stress, strain, and temperature.

Materials Sciences Corporation

ELEVATED TEMPERATURE BEHAVIOR OF METAL-MATRIX COMPOSITES

Technical Final Report
MSC TFR 1214/1502
November, 1981

Prepared by:
Zvi Hashin and E. A. Humphreys

Prepared for:
Air Force Office of Scientific Research
Bolling Air Force Base, D.C.

Gwynedd Plaza II, Bethlehem Pike, Spring House, PA • 215-542-8400

TECHNICAL FINAL REPORT
April 1, 1979 - September 30, 1981

The present report summarizes the research effort by the Materials Sciences Corporation on the analysis of temperature-dependent stress-strain relations of metal-matrix composites (MMC) during the period April 1, 1979 through September 30, 1981. The work done is part of a comprehensive program to provide analytical tools for the evaluation of thermomechanical properties and internal stresses of unidirectional MMC. This program consisted of the following parts:

1. Analytical determination of one-dimensional temperature dependent stress-strain relations on the basis of micromechanics.
2. Determination of temperature-dependent stress-strain relations for combined states of stress in terms of one-dimensional stress-strain relations on the basis of macro-incremental theory.

TABLE OF CONTENTS

INTRODUCTION

The usual unidirectional metal matrix composite (MMC) consists of an aluminum alloy matrix and aligned carbon, graphite or boron fibers. The metal matrix is a temperature dependent elasto-plastic isotropic material. The fibers are anisotropic elastic throughout the temperature range but their properties may be temperature dependent. They may be described as transversely isotropic elastic with respect to their longitudinal axes.

Metal matrix composites are considerably more expensive than polymer matrix composites. The main reasons for their development are their better retention of strength and stiffness at elevated temperatures. For purposes of efficient designs with such composites, their mechanical behavior must be quantitatively known. The composite is evidently an anisotropic temperature dependent elasto-plastic material. Consequently, all applied stresses and temperatures will produce interactive non-superposable deformations. In addition, the composite is history dependent. This implies that different loading histories resulting in the same end state (e.g. axial load-torsion-heating, torsion-axial load-heating, etc.) will produce different deformations. It follows that an experimental program to define the stress-strain relations would require an enormous number of experiments and the interpretation of the results would be extremely difficult.

Another alternative is to devise an analytical treatment for determination of the stress-strain relations. This, however, also involves severe difficulties. Analysis of any model of a fiber composite can only be carried out numerically and the amounts of computer time required make such procedures quite expensive. It is in principle possible, as will be shown in this work, to carry out such numerical analyses for any load-temperature program but here there arises the same difficulty

as with the experimental program. The number of variables is large and load-temperature histories are of infinite variety. Thus, purely numerical analysis is as expensive and as futile as purely experimental investigation.

A possible solution to these difficulties is to restrict numerical analysis to simple loading cases in which only one stress component is applied, e.g. simple tension or pure shear, and to establish a global theory for the stress-strain relations for complicated loadings which incorporates the information contained in the one dimensional stress-strain relations, obtained numerically. (Such a global theory can also be based on experimentally obtained one dimensional stress-strain relations.) This method will be followed in the present work.

The problem of the analytical determination of elasto-plastic stress-strain relations has received repeated attention in the literature. A general qualitative discussion of elasto-plastic composites has been given in reference 1. Limit analysis treatments which are only concerned with prediction of ultimate loads for ideally plastic matrix have been given in references 2 and 3. A numerical treatment to compute the stress-strain relation for transverse uniaxial stress for a limited strain range has been given in reference 4 based on the idealized geometry of a square array fiber model. A similar approach but including interaction between shear and transverse load has been given in reference 5. A micromechanics stress analysis for a square array has been given in reference 6. The self-consistent scheme approximation has been utilized in reference 7 for the case of rigid fibers and elasto-plastic matrix characterized by isotropic J_2 deformation theory. This was generalized in reference 8 to include fiber elasticity; all this for transverse loading only. Significan work to predict initial yield surfaces has been given in references 9, 10, 11 and 12, including temperature change but primarily for axisymmetric states. The general form of the elasto-plastic isothermal stress-strain relations of a unidirec-

tional fiber composite consisting of elastic isotropic fibers and ideally plastic matrix has been discussed in reference 13.

All of the treatments available describe important special cases but they are not sufficient to define the needed temperature dependent stress-strain relations of a unidirectional MMC, neither for the one dimensional nor for the three dimensional case.

The following investigation is divided into three main parts. In the part METHOD OF ANALYSIS: ONE DIMENSIONAL EFFECTIVE STRESS-STRAIN RELATIONS, we formulate the elasto-plastic problem of the hexagonal array of fibers in terms of two kinds of two dimensional boundary value problems for typical repeating elements. This formulation is then used to numerically obtain effective temperature dependent stress-strain relations for one dimensional loadings such as transverse tension, transverse shear and axial shear by means of the ANSYS computer code.

In the part THREE DIMENSIONAL STRESS-STRAIN RELATIONS. ISOTHERMAL CASE, we use global plasticity considerations to construct isothermal incremental stress-strain relations of a transversely isotropic unidirectional fiber composite in terms of known one dimensional stress-strain relations.

Finally, in the part TEMPERATURE DEPENDENT STRESS-STRAIN RELATIONS, we extend these results to temperature changes resulting in a set of effective stress-strain relations incremental in stress, strain and temperature.

METHOD OF ANALYSIS: ONE DIMENSIONAL EFFECTIVE STRESS-STRAIN RELATIONS

When a homogeneous body consisting of elasto-plastic material is subjected to the traction rate boundary conditions

$$\dot{T}_i^o(S) = \dot{\sigma}_{ij}^o n_j \tag{2.1}$$

where $\dot{\sigma}_{ij}^o$ are space constant stress rates and n_j are components of the outward unit normal, the stress rates throughout are the constant $\dot{\sigma}_{ij}^o$. If (2.1) are applied to the surface of an elasto-plastic heterogeneous body, such as the fiber composite under consideration here, it follows from the average stress rate theorem (ref. 14) that average stress rates are given by

$$\dot{\bar{\sigma}}_{ij} = \dot{\sigma}_{ij}^o . \tag{2.2}$$

If the internal phase geometry of the component is statistically homogeneous, the stress and strain fields associated with (2.1) are also statistically homogeneous. Then (2.2) can be interpreted in terms of averages over a representative volume element (RVE).

Now let the body be subjected to the constant boundary temperature rate

$$\dot{\phi}(S) = \dot{\phi}_o(S) . \tag{2.3}$$

It follows trivially from the equations of steady state uncoupled heat conduction that the temperature rate field throughout the heterogeneous body is the constant $\dot{\phi}_o$ and thus the temperature is space constant at all times.

In a temperature dependent elasto-plastic material the relation between strain rates, stress rates and temperature rate is linear. It can be shown that if the constituents of a composite have this property, the same is true for the relation of average strain rates to average stress rates and temperature rate when the composite is subjected to (2.1) and (2.3). Therefore,

$$\dot{\bar{\varepsilon}}_{ij} = C^{*}_{ijkl}\dot{\bar{\sigma}}_{kl} + \beta^{*}_{ij}\dot{\theta} \qquad (2.4)$$

where C^{*}_{ijkl} and β^{*}_{ij} are complicated functions of average stress, strain and temperature history and of the internal phase geometry, but not of average stress rates, strain rates or temperature rate. The relations (2.4) are the effective stress-strain relations of the composite. Their form will be discussed later in this work. At present, attention will be directed towards stress-strain response for one dimensional temperature dependent loadings.

We now consider the specific case of a unidirectional fiber composite in the form of a long cylindrical specimen (figure 1). The matrix is temperature dependent, isotropic and elasto-plastic, and the fibers are elastic transversely isotropic. This is an appropriate description of aluminum matrix containing carbon or graphite fibers. To compute effective stress-strain relations, it is necessary to find the average strain rates produced by the average stress rates. This requires analysis of strain and stress rate fields subject to displacement and traction rate continuity at fiber/matrix interfaces, the analysis being carried out incrementally for specified external loading histories. Since the matrix is temperature dependent elasto-plastic, such analysis for any given model of a fiber composite can only be performed numerically.

All of the problems to be considered here can, fortunately, be formulated in two dimensions. For this purpose, let the strain rates (2.2) be split as follows

$$\dot{\varepsilon}^{\circ}_{ij} = \dot{\varepsilon}^{p}_{ij} + \dot{\varepsilon}^{a}_{ij} \tag{2.5}$$

$$[\dot{\varepsilon}^{p}_{ij}] = \begin{bmatrix} \dot{\varepsilon}^{\circ}_{11} & 0 & 0 \\ 0 & \dot{\varepsilon}^{\circ}_{22} & \dot{\varepsilon}^{\circ}_{23} \\ 0 & \dot{\varepsilon}^{\circ}_{23} & \dot{\varepsilon}^{\circ}_{33} \end{bmatrix} \qquad \text{(a)}$$

$$[\dot{\varepsilon}^{a}_{ij}] = \begin{bmatrix} 0 & \dot{\varepsilon}^{\circ}_{12} & \dot{\varepsilon}^{\circ}_{13} \\ \dot{\varepsilon}^{\circ}_{12} & 0 & 0 \\ \dot{\varepsilon}^{\circ}_{13} & 0 & 0 \end{bmatrix} \qquad \text{(b)} \tag{2.6}$$

It may be shown that when $\dot{\varepsilon}^{\circ}_{ij}$ in (2.1) have the form (2.6a), the problem of the determination of the stress and strain rates in fibers and matrix can be formulated in terms of generalized plane strain which implies that

$$\dot{\varepsilon}_{11} = \text{const} \qquad \text{(a)}$$

$$\dot{\varepsilon}_{\alpha\beta} = \dot{\varepsilon}_{\alpha\beta}(x_2, x_3) \qquad \text{(b)} \quad \alpha,\beta=2,3 \tag{2.7}$$

$$\dot{\varepsilon}_{12} = \dot{\varepsilon}_{13} = 0 \qquad \text{(c)}$$

in fibers and matrix. Such problems can be solved in terms of two dimensional stress rate fields with

$$\dot{\varepsilon}_{12} = \dot{\varepsilon}_{13} = 0 \ . \tag{2.8}$$

When $\dot{\sigma}^{\circ}_{ij}$ have the form (2.6b), the problem can be formulated in terms of anti-plane strain which implies that

$$\dot{\varepsilon}_{12} = \dot{\varepsilon}_{12}(x_2,x_3)$$
$$\dot{\varepsilon}_{13} = \dot{\varepsilon}_{13}(x_2,x_3) \tag{2.9}$$

and all other strain rates vanish. Such problems can be solved in terms of a two dimensional stress rate field for which

$$\dot{\varepsilon}_{11} = \dot{\varepsilon}_{22} = \dot{\varepsilon}_{33} = \dot{\varepsilon}_{23} = 0 \tag{2.10}$$

and thus only the two shear rates $\dot{\sigma}_{12}$ and $\dot{\varepsilon}_{13}$ remain, which are functions of x_2,x_3 only.

One dimensional loadings of interest are uniaxial average stress in the fiber direction, transverse uniaxial stress, transverse shear and axial shear. The first three all fall into category (2.6a) while the last is in category (2.6b). For stress in the fiber direction, when the fibers are high modulus carbon, graphite or boron, it may be safely assumed that the axial average strain $\bar{\varepsilon}_{11}$ is elastic since in this case fiber and matrix ε_{11} strains must be equal and the stiff fibers inhibit plastic matrix flow. In the other cases, however, substantial average plastic strains can develop as a consequence of matrix plasticity.

For the purpose of computation of effective stress-strain relations, it is necessary to describe the fiber composite by a suitable geometrical model. There exist, at the present time, only two kinds of models which permit exact analysis: (1) the composite cylinder assemblage (CCA) (refs. 14,15) shown in figures 2, 3 which has been employed successfully to find effective properties for various kinds of linear physical behavior, in closed analytical form, and (2) periodic arrays of identical circular fibers which have been analyzed numerically. Unfortunately, the CCA is only of limited usefulness for the present case of elasto-plastic temperature dependent matrix since it does not lend itself to evaluation of transverse normal or shear stressing while analysis of axial shearing would require complicated numerical procedures. Since the fiber composite is transversely isotropic in the macrosense, we shall choose as our model a hexagonal array of identical circular fibers. This model fulfils the necessary initial transverse isotropy requirements. Note that the model of a square array of circular fibers, which has often been used for modelling fiber reinforced materials, is not transversely isotropic and is, therefore, not suitable. Elastic analyses have shown that the CCA model and the hexagonal array give results which are numerically very close. This leads to the speculation that the results have wider applicability than the restricted nature of the model implies and are probably valid for any transversely isotropic arrangement of separated circular fibers.

The hexagonal array is shown in figure 4. A typical rectangular repeating element is indicated in the figure. The whole array can be built up of such elements and the states of stress and strain in these elements are identical. Actually

the rectangular element can be separated into two repeating triangular elements as shown in the figure, but for the purpose of analysis the rectangular element is more convenient.

GENERALIZED PLANE STRAIN

We first consider case (2.6a) for some constant temperature. Without loss of generality, this loading can be written as

$$[\dot{\sigma}^{\circ P}_{ij}] = \begin{bmatrix} \dot{\sigma}^{\circ}_1 & 0 & 0 \\ 0 & \dot{\sigma}^{\circ}_2 & 0 \\ 0 & 0 & \dot{\sigma}^{\circ}_3 \end{bmatrix} \tag{2.11}$$

where $\dot{\sigma}^{\circ}_2$, $\dot{\sigma}^{\circ}_3$ are the principal transverse stress rates. Because of the transverse isotropy of the model, the average strain rates produced by (2.11) do not depend on the direction of transverse axes and thus the principal axes can be taken as the Cartesian reference system.

It follows from symmetry that the deformed shape of the repeating rectangle remains a rectangle. Without loss of generality, the normal displacements of two adjoining sides may be taken as zero. Consequently, the rectangle is subject to the following boundary conditions on its contour C

$$\dot{\sigma}_{23(C)} = 0 \qquad \text{(a)}$$

$$\dot{u}_2(0,x_3) = 0 \qquad \dot{u}_2(a_2,x_3) = \eta_2 a_2 \qquad \text{(b)} \tag{2.12}$$

$$\dot{u}_3(x_2,0) = 0 \qquad \dot{u}_3(x_2,a_3) = \eta_3 a_3 \qquad \text{(c)}$$

The constants η_2, η_3 have a simple and important physical interpretation. Application of the average strain rate theorem (ref. 14) in the two dimensional version yields

$$\dot{\bar{\varepsilon}}_{ij} = \frac{1}{A} \int_C (\dot{u}_i n_j + \dot{u}_j n_i) ds \tag{2.13}$$

where A is the area of the rectangle. Consequently,

$$\begin{aligned} \eta_2 &= \dot{\bar{\varepsilon}}_{22} \\ \eta_3 &= \dot{\bar{\varepsilon}}_{33} \, . \end{aligned} \tag{2.14}$$

In order to define the boundary value for the rectangle, the parameters η_2 and η_3 must be expressed in terms of the stress rates (2.11). To do this, we exploit the rate linearity of rate independent plasticity. Suppose that the current states of displacement, strain and stress in the repeating rectangle are $\underline{u}$, $\underline{\varepsilon}$ and $\underline{\sigma}$. Now consider the two boundary value problems shown in figures 5a and 5b where each rectangle is in the same current state prior to displacement increment. If the solutions to these boundary value problems are identified by superscripts *I and II, it follows from rate linearity that*

$$\dot{\underline{u}} = \eta_2 \dot{\underline{u}}^I + \eta_3 \dot{\underline{u}}^{II} \qquad \text{(a)}$$

$$\dot{\underline{\varepsilon}} = \eta_2 \dot{\underline{\varepsilon}}^I + \eta_3 \dot{\underline{\varepsilon}}^{II} \qquad \text{(b)} \tag{2.15}$$

$$\dot{\underline{\sigma}} = \eta_2 \dot{\underline{\sigma}}^I + \eta_3 \dot{\underline{\sigma}}^{II} \qquad \text{(c)}$$

Define average stress rates

$$\dot{\bar{\sigma}}_{22} = \frac{1}{a_3}\int_0^{a_3} \dot{\sigma}_{22}\, dx_3$$

$$\dot{\bar{\sigma}}_{33} = \frac{1}{a_2}\int_0^{a_2} \dot{\sigma}_{33}\, dx_2 \,. \tag{2.16}$$

Since the states of stress/stress rate are the same in all repeating elements except for a boundary layer near the external boundary, it follows from equilibrium that the stress rates (2.16) are equal to (2.11). Then by averaging (2.15c)

$$\eta_2 \dot{\bar{\sigma}}^{I}_{22} + \eta_3 \dot{\bar{\sigma}}^{II}_{22} = \dot{\sigma}^{\circ}_2$$

$$\eta_2 \dot{\bar{\sigma}}^{II}_{33} + \eta_3 \dot{\bar{\sigma}}^{II}_{33} = \dot{\sigma}^{\circ}_3 \,. \tag{2.17}$$

This defines the constants η_2, η_3, i.e. the average strain rates in terms of stress averages obtained from the two boundary value problems and thus the solution (2.15) for the repeating rectangle is determined. Note that η_2, η_3 are functions of current state variables. Also note that (2.15-17) can be expressed in terms of increments instead of rates and would be used in this form in a numerical procedure. Once the increments $d\underline{u}$, $d\underline{\varepsilon}$ and $d\underline{\sigma}$ are known, they are added to the current state and the same solution procedure can be carried out again for new increments $d\sigma^{\circ}_1$ and $d\sigma^{\circ}_2$.

Note that because of the generalized plane strain formulation the solution includes the unknown constant strain rate $\dot{\varepsilon}_{11}$ (2.7a). This is found from the requirement that

$$\dot{\bar{\sigma}}_{11} = \dot{\sigma}_1^\circ = \frac{1}{A}\int_0^{a_2}\int_0^{a_3} \dot{\sigma}_{11}\, dx_2 dx_3 . \qquad (2.18)$$

The average shear rates $\dot{\bar{\sigma}}_{12}$ and $\dot{\bar{\sigma}}_{13}$ vanish identically since $\dot{\sigma}_{12} = \dot{\sigma}_{13} = 0$ in the generalized plane strain solution.

This procedure defines relations among the average stress rates $\dot{\bar{\sigma}}_{22}$, $\dot{\bar{\sigma}}_{33}$ and the average strain rates $\dot{\bar{\varepsilon}}_{22}$ and $\dot{\bar{\varepsilon}}_{33}$ at current states. It is thus, in principle, possible to obtain the average strains for specified average loading history in incremental fashion. If in particular $\bar{\sigma}_{33} = \sigma_{33}^\circ = 0$, then the procedure will define the effective stress-strain relation for uniaxial transverse stressing in the x_2 direction, which by the transverse isotropy is also the stress-strain relation for uniaxial stressing in the x_3 direction. The effective transverse tangent modulus E_{Tt}^* is defined by

$$E_{Tt}^*(\bar{\sigma}_{22}) = \frac{\dot{\bar{\sigma}}_{22}}{\dot{\bar{\varepsilon}}_{22}} = \frac{\dot{\sigma}_{22}^\circ}{\eta_2} .$$

To find the stress-strain relation in transverse shear, it is convenient to use the special case of (2.11)

$$\dot{\sigma}_2^\circ = -\dot{\sigma}_3^\circ$$

$$\dot{\sigma}_1^\circ = 0 .$$

This results in average strain rates

$$\dot{\bar{\varepsilon}}_{22} = \eta_2 = -\dot{\bar{\varepsilon}}_{33} .$$

An element rotated by 45° with respect to the x_2 axes will be in a state of average pure shear stress τ° and shear strain $\frac{1}{2}\bar{\gamma}$ defined by

$$\dot{\tau}^{\circ} = \dot{\sigma}^{\circ}_2$$

$$\tfrac{1}{2}\dot{\bar{\gamma}} = \dot{\bar{\varepsilon}}_{22} \quad .$$

Because of the transverse isotropy this also defines the tranverse shear stress strain relation in any set of transverse orthogonal axes.

Next we consider the case of an applied temperature rate $\dot{\phi}$ throughout the composite with all $\dot{\sigma}^{\circ}_{ij} = 0$ in (2.1) and (2.6). The symmetry is as before and the repeating rectangle is again subject to the boundary conditions (2.12) but because of the transverse isotropy the average strain rates in the x_2 and x_3 directions must be equal. Therefore, from (2.14)

$$\eta_2 = \eta_3 = \eta \quad . \tag{2.19}$$

The effective tangent thermal expansion coefficients <u>at the current state</u> are defined by

$$\begin{aligned} \dot{\bar{\varepsilon}}_{22} &= \dot{\bar{\varepsilon}}_{33} = \alpha^{*}_{Tt}\dot{\phi} \\ \dot{\bar{\varepsilon}}_{11} &= \alpha^{*}_{At}\dot{\phi} \end{aligned} \tag{2.20}$$

where T, A denote transverse and axial respectively. In general these expansion coefficients are functions of current stress, strain and temperature.

The basic boundary value problem for the repeating rectangle which must be solved is shown in figure 5c. The input is $\dot{\phi} = 1$. The average strain rates are determined from

$$\dot{\bar{\sigma}}_{22} = \dot{\bar{\sigma}}_{33} = 0 \tag{2.21}$$

utilizing (2.16), and the constant axial strain rate is found from

$$\dot{\bar{\sigma}}_{11} = 0 \tag{2.22}$$

utilizing (2.18). Because of (2.19-20) these strain rates are equal to the tangent thermal expansion coefficients.

Because of the rate linearity of the problems considered, loading (2.11) can be combined with heating to analyze by the same procedures effective stress-strain relations in the presence of change of temperature history.

ANTIPLANE STRAIN - AXIAL SHEARING

We now consider the axial shear loading (2.6b). Guided by the elastic formulation of the problem (ref. 14) we write the displacement rates in the form

$$\begin{aligned} \dot{u}_1(\underline{x}) &= \dot{\varepsilon}^{\circ}_{12}x_2 + \dot{\varepsilon}^{\circ}_{13}x_3 + \dot{\psi}(x_2,x_3) \\ \dot{u}_2(\underline{x}) &= \dot{\varepsilon}^{\circ}_{12}x_1 \\ \dot{u}_3(\underline{x}) &= \dot{\varepsilon}^{\circ}_{13}x_1 \,. \end{aligned} \tag{2.23}$$

It will be shown further below that $\dot{\varepsilon}^{\circ}_{12}$ and $\dot{\varepsilon}^{\circ}_{13}$ are the average strain rates in the fiber composite cylinder. The only non-vanishing strain rates associated with (2.23) are

$$\dot{\varepsilon}_{12} = \dot{\varepsilon}^{\circ}_{12} + \tfrac{1}{2}\dot{\psi}_{,2}$$

$$\dot{\varepsilon}_{13} = \dot{\varepsilon}^{\circ}_{13} + \tfrac{1}{2}\dot{\psi}_{,3} \; . \tag{2.24}$$

The strain rates (2.24) are equivalent to a principal shear strain rate

$$\dot{\varepsilon}^{2}_{p} = \dot{\varepsilon}^{2}_{12} + \dot{\varepsilon}^{2}_{13} \tag{2.25}$$

whose direction n is specified by

$$\tan\,(x_2,n) = \dot{\varepsilon}_{13}/\dot{\varepsilon}_{12} \; .$$

This will result in a principal shear stress rate in the same direction

$$\dot{\tau}_{p} = 2G_{t}\,\dot{\varepsilon}_{p} \tag{2.26}$$

where G_t is the tangent modulus. The stress (2.26) is equivalent to the Cartesian components

$$\dot{\sigma}_{12} = \dot{\tau}_{p}\cos(x_2,n)$$

$$\dot{\sigma}_{13} = \dot{\tau}_{p}\sin(x_2,n) \tag{2.27}$$

It follows that the only nonvanishing stress rates are the ones given above.

It may be shown that this formulation results in a well posed plasticity boundary value problem for stress and strain rates when the boundary conditions are of type (2.1) with (2.6b) i.e. axial shearing.

We consider the case of axial shearing in the 12 plane. The boundary conditions (2.1) then have the form

$$\begin{aligned} \dot{T}_1(S) &= \dot{\sigma}^{\circ}_{12} n_2 \\ \dot{T}_2(S) &= \dot{\sigma}^{\circ}_{12} n_1 \\ \dot{T}_3(S) &= 0 \ . \end{aligned} \tag{2.28}$$

The displacement formulation (2.23) then assumes the form

$$\begin{aligned} \dot{u}_1(\underline{x}) &= \dot{\varepsilon}^{\circ}_{12} x_2 + \dot{\psi}(x_2, x_3) \\ \dot{u}_2(\underline{x}) &= \dot{\varepsilon}^{\circ}_{12} x_1 \\ \dot{u}_3(\underline{x}) &= 0 \ . \end{aligned} \tag{2.29}$$

For the purpose of computation of the function ψ, it is necessary to establish its boundary conditions on the contour of a repeating element. Figure 6 shows four joined repeating elements. Evidently, ψ obeys the symmetry condition

$$\psi(x_2, x_3) = \psi(x_2, -x_3) \ . \tag{2.30}$$

It will be shown that it obeys an antisymmetry condition with respect to the x_2 axis. To see this, consider the two upper rectangles. If the direction of shear stress acting on any one, the right one say, were reversed, then these two rectangles would be in a symmetric state with respect to the x_2 axis. Reversing the direction of shear stress in the right side rectangle to conform with the actual situation reverses the sign of the field in this rectangle. The conclusion is that the fields are antisymmetric with respect to the x_2 axis, thus

$$\psi(x_2,x_3) = -\psi(-x_2,x_3) \ . \tag{2.31}$$

It follows from (2.28) that

$$\psi(0,x_3) = 0$$

and by the same reasoning

$$\psi(a_2,x_3) = 0 \ .$$

It follows from (2.27) that

$$\psi_{,3}(x_2,x_3) = -\psi_{,3}(x_2,-x_3)$$

and therefore

$$\psi_{,3}(x_2,0) = \psi_{,3}(x_2,a_3) = 0 \ .$$

Thus, the rate boundary conditions for ψ on the boundary of a repeating element are summarized as

$$\dot{\psi}(0,x_3) = \dot{\psi}(a_2,x_3) = 0 \qquad \text{(a)}$$

$$\dot{\psi}_{,3}(x_2,0) = \dot{\psi}_{,3}(x_2,a_3) = 0 \; . \qquad \text{(b)} \tag{2.32}$$

The second boundary condition is inconvenient for finite element applications. An alternative condition is

$$\dot{\sigma}_{13}(x_2,0) = \dot{\sigma}_{13}(x_2,a_3) = 0 \tag{2.33}$$

which is again a consequence of the fact that x_2 must be an axis of symmetry.

At the fiber matrix interfaces, C_{12}, displacements and tractions must be continuous. This implies from (2.29) that

$$\dot{\psi}_m(C_{12}) = \dot{\psi}_f(C_{12}) \tag{2.34}$$

where m and f denote fibers and matrix. It follows from (2.27) that the only nonvanishing traction rate component on C_{12} is

$$\dot{T}_1 = \dot{\sigma}_{12}n_2 + \dot{\sigma}_{13}n_3$$

where n_2,n_3 are components of the normal to C_{12}. Thus, the second continuity condition is

$$\dot{T}_{1m}(C_{12}) = \dot{T}_{1f}(C_{12}) \tag{2.35}$$

To show that $\dot{\varepsilon}^{\circ}_{12}$ is the average strain rate, we recall the average strain rate theorem (ref. 14) which states that

$$\dot{\bar{\varepsilon}}_{ij} = \frac{1}{2V}\int_S (\dot{u}_i n_j + \dot{u}_j n_i)\,dS \tag{2.36}$$

where V is the volume and S the surface. Applying this to a repeating element of unit thickness in the x_1 direction, figure 4, for the strain ε_{12} we have

$$\dot{\bar{\varepsilon}}_{12} = \frac{1}{2a_2a_3}\int_S (\dot{u}_1 n_2 + \dot{u}_2 n_1)\,dS \tag{2.37}$$

where n_1, n_2 are the components of the outward normal in the 1, 2 directions. It is seen that n_1 vanishes on the enclosing faces while n_2 vanishes on the upper and lower faces and on the faces $x_3 = 0, a_3$. We introduce (2.29) into (2.37) recalling the boundary conditions (2.32a). Without loss of generality the x_1 origin may be taken at the bottom face which makes $\dot{u}_2$ vanish on this face. As a result of all this

$$\dot{\bar{\varepsilon}}_{12} = \frac{\dot{\varepsilon}^\circ_{12}}{2a_2a_3}\left[\int_0^{a3} a_2 dx_3 + \int_0^{a2}\int_0^{a3} dx_2 dx_3\right] = \dot{\varepsilon}^\circ_{12}\,. \tag{2.38}$$

In view of (2.21) the only nonvanishing average stress rate for the loading (2.28) is

$$\dot{\bar{\sigma}}_{12} = \dot{\sigma}^\circ_{12} \tag{2.39}$$

The relation between the average strain and stress rates (2.38-39) defines the stress strain relation of the fiber composite in axial shear. To obtain this relation numerically, we start from some known state of stress and strain in the composite e.g. elastic. We impose a strain increment $\Delta\varepsilon^\circ_{12}$ and write all rate equations as increments. This defines a $\Delta\psi$ and stress and strain increments $\Delta\sigma_{12}$, $\Delta\sigma_{13}$, $\Delta\varepsilon_{12}$ and $\Delta\varepsilon_{13}$. These are computed by numerical

solution of the plasticity problem for the repeating element subject to boundary and interface conditions (2.32-35) for increments. The resulting stress increment $\Delta\sigma_{12}$ is proportional to $\Delta\bar{\varepsilon}^{\circ}_{12}$. Its average $\Delta\bar{\sigma}_{12}$ defines the average stress increment corresponding to an average strain increment $\Delta\bar{\varepsilon}^{\circ}_{12}$. The procedure is repeated for other strain increments and thus the stress-strain relation is obtained in step wise fashion.

The procedures described in this section permit, in principle, analysis of stress and strain states in the hexagonal array model for any kind of loading and temperature change as specified by (2.1), (2.3) by numerical solution of rate value problems for one repeating element for isothermal generalized plane strain, thermal input with no load, and axial shear. Because of rate linearity the rate fields can be superposed at any current state and, therefore, any loading and temperature variation history can be treated. Actual execution of a solution may involve very considerable computer expenses. Therefore, the procedures are applied in this work only to one dimensional average loadings such as uniaxial stress and pure shear. The problem of determination of effective stress-strain relations for arbitrary loadings will be considered in section 3 by different methods.

NUMERICAL RESULTS

The analytical models developed and described in the previous section were utilized in conjunction with an elasto-plastic, temperature dependent finite element analysis to predict one dimensional stress-strain responses for a metal matrix composite. The loadings considered included tranverse normal stresses, transverse shear stresses, axial shear stresses and uniform temperature variations. The composite considered was a T-50 graphite

fiber in a 2024-T4 aluminum alloy. The fiber volume fraction was 30%.

The finite element code utilized was ANSYS, which is a proprietary analysis code developed by Swanson Analysis Systems Inc. (ref. 16). A description of the formulation of the plasticity relations utilized in ANSYS can be found in Appendix A.

The elastic material constants used in the analysis performed for the fiber and matrix are shown in table 1. The fiber properties correspond to a Union Carbide T-50 graphite fiber. The matrix properties are representative of a 2024-T4 aluminum alloy.

The finite element model utilized for the numerical analysis is shown in figure 7. The validity and accuracy of this model was demonstrated both numerically and analytically.

The method used for assessing the accuracy of the finite element model involved predicting elastic moduli of the unidirectional composite. The moduli were computed by applying loads (stresses) to the model and finding the resultant displacements (strains). The boundary conditions used corresponded to the symmetry conditions described previously.

Elastic moduli predicted by a finite element analysis were compared with composite cylinder assemblage results. The comparisons are shown in table 2. As can be seen, excellent agreement between the two models was demonstrated. Additionally, a comparison of the results predicted with the finite element model shown in figure 7 and a considerably more refined finite element model was made. The refined model contained approximately twice the number of elements and nodal points shown in figure 7. The differences in predicted elastic moduli were of the order of 0.5%, thus again demonstrating the accuracy of the finite element mesh.

The prediction of stress-strain relations for the metal matrix composite under consideration requires that full stress-strain relations for the constituent materials be utilized. In the case of graphite fibers, in the temperature ranges to be considered, these relations are linearly elastic and temperature independent. Hence, only the room temperature elastic constants are required. The aluminum matrix material is considerably different, however.

The aluminum matrix is elasto-plastic and temperature dependent. The way in which this is modelled in ANSYS depends upon the material strain hardening rule desired. If isotropic hardening is desired, the stress-strain response of the material must be represented as linearly segmented curves at various temperatures. The representation used for isotropic hardening in the current study is shown in figure 8.

ANSYS requires a different form of the stress-strain relations if kinematic hardening is desired. Here only two linear segments are allowed for each of the various temperatures. The kinematic hardening data used in the current study is shown in figure 9.

In addition to the stress-strain response, thermal expansion coefficients are required. A curve representing the secant thermal expansion coefficient as a function of temperature for the aluminum matrix is shown in figure 10.

Utilizing the finite element model, boundary conditions and material properties described, various one dimensional stress-strain responses were predicted. Additionally, thermal expansion coefficients were predicted. These results are described here in some detail as they demonstrate many interesting features of metal matrix composites.

Thermal Expansion

The free thermal response of the T-50/2024-T4 material system is depicted in figures 11 and 12. The responses utilizing both

isotropic and kinematic hardening for the aluminum matrix are shown. The curves represent a thermal cycle from the stress-free temperature to room temperature and back to the stress-free temperature.

The states of microscopic stress and strain which exist at room temperature can involve considerable matrix yielding. This effect is clearly demonstrated by comparing the decreasing temperature response to the increasing temperature response. In both the isotropic and kinematic hardening solutions, the re-heat is totally elastic at the lower end of the temperature scale. The differences between the cool-down and re-heat curves at these low temperatures corresponds to the matrix plasticity developed during cool-down.

At higher temperatures in the re-heat portion of the curves, the differences between the two hardening assumptions are apparent. The isotropic hardening predictions remain elastic up to the stress-free temperature due to the expansion of the yield surface during cool-down. The kinematic prediction involves additional yielding upon re-heating since this hardening assumption shifts the yield surface rather than expanding it. Thus, the re-heat caused the microscopic matrix stresses to extend beyond the shifted yield stress space.

The minor differences between the two loading assumptions during the cooling cycle are due entirely to the different material representations required by ANSYS for the two hardening assumptions.

The effects of applied mechanical loading on the thermal expansion of this metal matrix system are demonstrated in figures 13 and 14. The matrix hardening assumption used for these predictions was isotropic. The reference state of stress and strain for these predictions includes the effects of cooling from the stress-free temperature to room temperature and, hence, matrix yielding has occurred.

In figures 13 and 14, the effects of applied mechanical loading on thermal expansion are shown. The figures compare free thermal expansion strains with thermal strains developed in the presence of an applied, constant stress in the x_2 direction. In each of the figures, the curves have been shifted such that zero strains are depicted at room temperature.

Figure 13 demonstrates the effects of the mechanical loading on transverse expansion. Here, the mechanical load produces an increased thermal expansion in the loading direction and a decreased thermal expansion perpendicular to the mechanical load. The same effect is seen in figure 14. The applied mechanical load produces a decrease in the axial thermal expansion.

One Dimensional Mechanical Loadings

The effects of processing stresses were graphically depicted in figures 11 and 12 where the thermal loading curves differ from the thermal unloading curves. This effect is also clearly present in the mechanical stress-strain response of this material system.

The effects of processing on transverse extensional loadings are shown in figures 15, 16 and 17. The three curves in each of these figures represent transverse tension and compression with processing stresses and transverse tension from a microscopically stress-free state. Figure 15 represents the stress-strain response while figures 16 and 17 depict Poisson induced strains.

In figure 15, the differences between tensile and compressive loadings with processing stresses are attributable to the sign of the residual processing stresses. The tensile loading produces some micro-level elastic unloading at low load levels while the compressive load produces only increased micro-level plastic loading. Hence, the tensile stress-strain response is stiffer and has a higher yield stress. The tensile loading curve without

residual stress depicts the same initial modulus as the tensile with processing response but with a much higher yield stress. This is due to large built in stresses when processing effects are included.

The Poisson induced strains in figure 16 show little difference between tension and compression with residual stresses while the curve which does not contain processing effects is significantly different. This is primarily because the tensile load without processing is nearly elastic.

The axial Poisson strains (fig. 17) show a very curious trend. While the solution without processing is again nearly elastic, the tensile loading curve with processing has a reversal in slope. This is again a function of the sign of the processing effects. The applied tensile load produces a contraction axially. The residual stresses are large and compressive in the fibers. Thus, as the applied load causes further matrix yielding, the matrix modulus decreases and the fibers expand axially relieving some of the residual compressive load. This produces the effect shown in figure 12. The same rationale with axial expansion rather than contraction due to the applied load produces the large strains under compressive loading.

Thermal Effects on Transverse Extension

The stress-strain response of Gr/Al can be expected to vary with temperature since the aluminum matrix is temperature dependent. This is clearly demonstrated in figures 18 and 19. The initial state for this applied x_2 direction extension contains the residual processing stresses and therefore the effects of processing and elevated temperature are present.

In figure 18, the effect of elevated temperature is seen in the reduced initial modulus at 204°C. The effects of processing combined with the elevated temperature are seen in the increased yield stress at 204°C. The increase in yield stress is a consequence of the reduction of processing induced stresses as the

temperature increases. Thus, while the response at room temperature is producing considerable matrix yielding in addition to that present from processing, the response at 204°C requires substantial additional load to re-load the matrix to the yield stress levels.

The effects seen in the Poisson induced strains are similar. At the higher temperature, the reversal in slope in the axial Poisson strain is not present, while the transverse Poisson strain at 204°C is substantially reduced in comparison to the room temperature response.

Effects of Temperature on Transverse Shear Response

The stress-strain response for Gr/Al for applied transverse shear loading is depicted in figure 20 for three values of uniform temperature. These predictions were each made from a microscopically stress-free state and as such do not include any processing effects.

These data clearly show the effects of decreasing matrix modulus and yield stress with increasing temperature.

Comparisons of the effects of processing effects on elevated temperature transverse shear response are contained in figure 21. Here, the presence of residual micro-level stresses are seen to alter the predicted response considerably. The initial yield stress has been reduced nearly to zero in both the room temperature and 260°C responses. The initial elastic portions of the curves are extremely limited when the residual stresses are included but do exhibit the same slope as the solutions without processing stresses.

It is most interesting that the processing stresses in conjunction with the effects of elevated temperature do not promote an increased yield strength at the elevated temperature as was seen in the transverse extension loadings (fig. 18). The reason that this effect is not seen in the transverse shear loading relates to the elastic modulus at the elevated temperature. In the shear solution, the elevated temperature was 260°C while the

extensional solution (fig. 18) elevated temperature was only 204°C. Noting figure 8, the elastic matrix modulus is significantly lower at 260°C than at 204°C. Thus, the material reaches the yield strain (Appendix A) at a much lower stress value at 260°C.

Effects of Temperature on Axial Shear Response

The axial shear stress-strain relationships for this Gr/Al system at three different uniform temperatures are shown in figure 22. These predictions were made from a microscopically stress-free state and, hence, contain no processing effects. The results are typical of elevated temperature response of a homogeneous material where the modulus and yield stress decrease with elevated temperature. The axial shear solutions were made without processing effects since this would have required a full three dimensional analysis. This complication is not a function of the analytical formulations. It relates to the operation of the analysis code used.

Load Path Effects

In order to determine the effects of path dependence of the material system under consideration, a number of analyses were made utilizing different paths to obtain identical final load states. These included combinations of load and temperature as well as combinations of bi-axial loading.

Comparisons of different load-temperature paths are shown in tables 3 through 5. Tables 3 and 4 were generated using the isotropic hardening assumption and tensile and compressive transverse loadings respectively.

In table 3, the data indicate that relatively low loadings produce less path dependence than higher loadings. This is, of course, to be expected, since the higher loadings produce more plastic effects. The data presented also indicate that in the range of loadings considered, superposition of mechanical

and thermal loadings would produce reasonable accuracy. This would be of tremendous significance in simplifying the analysis of this material.

The data in table 4 demonstrate trends similar to the table 3 data. Here, as in the higher tensile loads data, the axial strain data show significant path dependence. The magnitudes of the strains are very small, however, and the differences may be exaggerated by the numerical errors inherent in the solution process.

The effects of path dependence with the kinematic hardening assumption were also evaluated for transverse tensile loadings and temperature. The comparison of the load path effects is listed in table 5. The differences here tend to be larger than for similar comparisons made for isotropic hardening (table 3). The difference of 15% in ε_2 is significant in that superposition of mechanical and thermal effects is probably not reasonable for these kinematic data.

The comparisons made here have shown *significant dependence* of the composite material response on the hardening assumptions for the matrix material when mechanical and thermal loadings are considered.

A final evaluation of path dependence was made utilizing a bi-axial transverse stress state and isotropic hardening. The results of this comparison are shown in table 6.

The load path effects seen in table 6 are considerably smaller than the combinations of temperature and load with the exception of the ε_1 data. As before, however, the magnitude of the ε_1 strains are very small in comparison to the transverse strain components and can, therefore, be expected to be computed less accurately. Thus, it is apparent that mechanical loading alone does not promote any significant path dependence.

THREE DIMENSIONAL STRESS-STRAIN RELATIONS. ISOTHERMAL CASE

In the present part of the work, the problem of establishment of the three dimensional stress-strain relations is considered in a global sense on the basis of the transverse isotropy of the material. A set of simplified effective stress-strain relations is established which exploits given one dimensional stress-strain relations obtained either numerically such as the ones derived in I, or experimentally. Thus, the heterogeneous structure of the composite enters indirectly via these one dimensional stress-strain relations.

The matrix is an elastic plastic temperature dependent material. The usual assumption is made that the strain increment d_{ij} is composed of an elastic part $d\varepsilon'_{ij}$, a plastic part $d\varepsilon''_{ij}$ and a thermal expansion increment $d\varepsilon_{ij}^{\phi}$. Thus

$$d\varepsilon_{ij} = d\varepsilon'_{ij} + d\varepsilon''_{ij} + d\varepsilon_{ij}^{\phi} \tag{3.1}$$

where

$$d\varepsilon'_{ij} = S_{ijkl} d\sigma_{kl} \tag{3.2}$$

$$d\varepsilon''_{ij} = g \frac{\partial F}{\partial \sigma_{ij}} dF \qquad dF \geq 0$$

$$dF = \frac{\partial F}{\partial \sigma_{kl}} d\sigma_{kl} + \frac{\partial F}{\partial \phi} d\phi \tag{3.3}$$

$$d\varepsilon''_{ij} = 0 \qquad dF<0$$

$$d\varepsilon_{ij}^{\phi} = \alpha_{ij} d\phi \tag{3.4}$$

where

$S_{ijkl}(\phi)$ - temperature dependent elastic compliances

$g = g(\underline{\sigma}, \underline{\varepsilon}, \phi)$

$F = F(\underline{\sigma}, \underline{\varepsilon}, \phi) = 1$ - the yield function

$\alpha_{ij}(\underline{\sigma}, \underline{\varepsilon}, \phi)$ - tangent thermal expansion coefficients; dependent on stress, strain and temperature.

It is seen that the matrix stress-strain relations can be written in the form

$$d\underline{\varepsilon} = \underline{R}(\underline{\sigma}, \underline{\varepsilon}, \phi) d\underline{\sigma} + \underline{\eta}(\underline{\sigma}, \underline{\varepsilon}, \phi) d\phi \tag{3.5}$$

The fibers are temperature dependent elastic transversely isotropic. Their stress-strain relations are

$$d\varepsilon_{11} = \frac{d\sigma_{11}}{E_A} - \frac{\nu_A}{E_A} d\sigma_{22} - \frac{\nu_A}{E_A} d\sigma_{33} + \alpha_A d\phi$$

$$d\varepsilon_{22} = -\frac{\nu_A}{E_A} d\sigma_{11} + \frac{d\sigma_{22}}{E_T} - \frac{\nu_T}{E_T} d\sigma_{33} + \alpha_T d\phi$$

$$d\varepsilon_{33} = -\frac{\nu_A}{E_A} d\sigma_{11} - \frac{\nu_T}{E_T} d\sigma_{22} + \frac{d\sigma_{33}}{E_T} + \alpha_T d\phi$$

$$d\varepsilon_{12} = d\sigma_{12}/2G_A \tag{3.6}$$

$$d\varepsilon_{23} = d\sigma_{23}/2G_T$$

$$d\varepsilon_{13} = d\sigma_{13}/2G_A$$

where

1 - fiber axial direction

2, 3 - transverse direction

E_A - axial Young's modulus

ν_A - associated axial Poisson's ratio

E_T - transverse Young's modulus

ν_T - associated transverse Poisson's ratio

G_T - $E_T/2(1+\nu_T)$ - transverse shear modulus

G_A - axial shear modulus

α_A - axial tangent thermal expansion coefficient

α_T - transverse tangent thermal expansion coefficient

All of the above properties are temperature dependent.

Consider a large cylindrical specimen of a fiber composite, with the fibers aligned in generator direction x_1, at current constant temperature ϕ and under current load defined by the boundary tractions

$$T_i(S) = \sigma^\circ_{ij} n_j \qquad (3.7)$$

where σ°_{ij} are space constant stresses and n_j the components of the outward unit normal. The average stresses in the cylinder are then (ref. 14)

$$\bar{\sigma}_{ij} = \sigma^{\circ}_{ij} \ . \tag{3.8}$$

However, the detailed states of stress and strain as well as the average strains are functions of the loading history culminating in (3.7).

Suppose that there are added a temperature increment $d\tau$ and boundary traction increments

$$dT_i(S) = d\sigma^{\circ}_{ij} n_j \tag{3.9}$$

then

$$d\bar{\sigma}_{ij} = d\sigma^{\circ}_{ij} \ . \tag{3.10}$$

Since the stress-strain relations (3.5-6) of the phases and their other governing equations are linear in stress, strain and temperature increments, it follows that the average strain increments in the cylinder are linearly related to the temperature increment and to $d\sigma^{\circ}_{ij}$ thus to $d\bar{\sigma}_{ij}$. These relations involve coefficients which are functions of the current state. It will be assumed that the current state and stress and strain enter through their averages. Thus

$$d\underline{\bar{\varepsilon}} = \underline{R}^*(\underline{\bar{\sigma}}, \underline{\bar{\varepsilon}}, \phi)\, d\underline{\bar{\sigma}} + \underline{p}^*(\underline{\bar{\sigma}}, \underline{\bar{\varepsilon}}, \phi)\, d\phi \ . \tag{3.11}$$

It is furthermore assumed that the usual plasticity concepts apply to the average states. Thus, the average strain increment can be separated as (3.1-4). It appears reasonable to require that g now become a tensor since the material is anisotropic. Consequently (3.11) is written in form similar to (3.5). Thus

$$d\bar{\varepsilon}_{ij} = S^*_{ijkl} d\bar{\sigma}_{kl} + g_{ijmn} \frac{\partial F}{\partial \bar{\sigma}_{mn}} dF \qquad \text{(a)}$$

$$+ \alpha^*_{ij} d\phi$$

(3.12)

$$dF = \frac{\partial F}{\partial \bar{\sigma}_{ij}} d\bar{\sigma}_{ij} + \frac{\partial F}{\partial \phi} d\phi \geq 0 \qquad \text{(b)}$$

while elastic unloading occurs when $dF < 0$. Here S^*_{ijkl} are the temperature dependent effective elastic compliances of the composite. Since the composite is transversely isotropic, they are defined by stress-strain relations of type (3.6) between average strain increments $d\bar{\varepsilon}_{ij}$ and average stress increments $d\bar{\sigma}_{ij}$ with effective properties, E^*_A, ν^*_A, etc. The yield function F depends in general on average stress, strain and strain hardening parameters. The functions g_{ijmn} depend in general on average stress and strain history and α^*_{ij} are the temperature dependent effective tangent thermal expansion coefficients. In the following, overbars denoting average stress and strain will be omitted.

In order to establish explicit stress-strain relations a number of simplifying assumptions will be made:

(1) The average plastic strain ε''_{11} in the fiber direction is negligible: The basis for this assumption is the large stiffness of the elastic fibers which inhibit plastic matrix strain in the fiber direction Thus

$$\varepsilon''_{11} = 0 \ . \qquad (3.13)$$

(2) The average stress σ_{11} in the fiber direction does not change the state of plastic average strain: The basis for this assumption is the same as above.

(3) The plastic volume change of the matrix is negligible.

(4) The composite is initially transversely isotropic and so remains during plastic flow: The second part of this assumption cannot be literally true but the alternative induces prohibitive difficulties.

(5) The yield function F depends on average stress and on temperature.

(6) The g_{ijmn} are functions of average stress and of temperature.

In the following we shall establish a specific set of stress-strain relations for the isothermal case. We shall then proceed in the next section to discuss temperature dependence. Since the fibers are elastic, it follows from (3) that

$$\varepsilon''_{11} + \varepsilon''_{22} + \varepsilon''_{33} = 0$$

and therefore from (1)

$$\varepsilon''_{22} + \varepsilon''_{33} = 0 \ . \qquad (3.14)$$

From (3.12) the average plastic strain increment is

$$d\varepsilon''_{ij} = g \frac{\partial F}{\partial \sigma_{ij}} dF \qquad (3.15)$$

It follows from (3.13-14) that

$$\frac{\partial F}{\partial \sigma_{11}} = 0 \qquad \text{(a)}$$

$$\frac{\partial F}{\partial \sigma_{22}} + \frac{\partial F}{\partial \sigma_{33}} = 0 \, . \qquad \text{(b)} \tag{3.16}$$

We temporarily introduce the stress variables

$$s = \tfrac{1}{2}(\sigma_{22} + \sigma_{33})$$

$$t = \tfrac{1}{2}(\sigma_{22} - \sigma_{33}) \, . \tag{3.17}$$

Transforming (2.16b) in terms of these variables we have

$$\frac{\partial F}{\partial s} = 0 \, . \tag{3.18}$$

Therefore and in view of (3.16a) the yield function must have the form

$$F = F[\tfrac{1}{2}(\sigma_{22}-\sigma_{33}), \sigma_{12}, \sigma_{23}, \sigma_{13}] \, . \tag{3.19}$$

The assumption of transverse isotropy (4) implies that the yield function depends on average stress in terms of its invariants with respect to an arbitrary rotation around the x_1 axis. These invariants are (ref. 13)

$$I_1 = \sigma_{11}$$

$$I_2 = \sigma_{22} + \sigma_{33} \tag{3.20}$$

$$I_3 = \tfrac{1}{4}(\sigma_{22}-\sigma_{33})^2 + \sigma_{23}^2$$

$$I_4 = \sigma_{12}^2 + \sigma_{13}^2 \qquad (3.20)\ \text{Cont'd}$$

$$I_5 = \tfrac{1}{2}(\sigma_{22}-\sigma_{33})(\sigma_{13}^2-\sigma_{12}^2) + 2\sigma_{12}\sigma_{23}\sigma_{13} \ .$$

It follows from (3.19-20) that

$$F = F(I_3, I_4, I_5) \ . \qquad (3.21)$$

A similar conclusion has been reached in reference 13. The specific nature of the functional dependence of (3.21) on the invariants is not known. We shall make the usual assumption that F is a quadratic function of average stress. This is consistent with the Mises yield function of isotropic plasticity and the Hill yield function of orthotropic plasticity. This eliminates I_5 since it is a cubic and leads to the form

$$F = I_3/\tau_T^2 + I_4/\tau_A^2 = 1 \qquad (3.22)$$

where τ_T and τ_A are two temperature dependent constants with dimension of stress which change with the loading. It is seen that I_3 and I_4 appearing in (3.22) are the squares of the principal shear stresses in the transverse x_2x_3 plane and the axial plane in the x_1 direction, respectively. Hence, the initial yield surface is

$$I_3/\tau_{To}^2 + I_4/\tau_{Ao}^2 = 1 \qquad (3.23)$$

where τ_{To} and τ_{Ao} are the initial transverse and axial shear yield stresses, respectively.

If it is further assumed that the yield function grows in stress space in self similar fashion, which is the analogue of the isotropic hardening assumption for initially isotropic materials, then

$$\frac{\tau_T}{\tau_{To}} = \frac{\tau_A}{\tau_{Ao}} \tag{3.24}$$

from which it follows that

$$\tau_T = \tau_{To}\sqrt{I_3/\tau_{To}^2 + I_4/\tau_{Ao}^2} \qquad \text{(a)}$$

$$\tau_A = \tau_{Ao}\sqrt{I_3/\tau_{To}^2 + I_4/\tau_{Ao}^2} \qquad \text{(b)} \tag{3.25}$$

In order to define the stress-strain relations it is necessary to determine the forms of the functions g_{ijmn} appearing in (3.12). The plastic strain increments as defined by these equations are given by

$$d\varepsilon''_{ij} = g_{ijmn}\frac{\partial F}{\partial \sigma_{mn}}\, dF \tag{3.26}$$

It is recalled that the composite is assumed to be transversely isotropic throughout the process of elasto-plastic deformation. Since the elastic and the free thermal parts of the strain increment obey transverse isotropic symmetry separately such symmetry must also be valid for the plastic strain increment (3.26). Recalling that the yield function F is not a function of σ_{11} the transversely isotropic form of (3.26) can be written as

$$d\varepsilon''_{11} = 0$$

$$d\varepsilon''_{22} = \left(g_{2222}\frac{\partial F}{\partial \sigma_{22}} + g_{2233}\frac{\partial F}{\partial \sigma_{33}}\right) dF \tag{3.27}$$

$$d\varepsilon''_{33} = (g_{3322}\frac{\partial F}{\partial \sigma_{22}} + g_{3333}\frac{\partial F}{\partial \sigma_{33}})\, dF$$

$$d\varepsilon''_{23} = 2g_{2323}\frac{\partial F}{\partial \sigma_{23}}\, dF \qquad (3.27)\ \text{Cont'd}$$

$$d\varepsilon''_{12} = 2g_{1212}\frac{\partial F}{\partial \sigma_{12}}\, dF$$

$$d\varepsilon''_{13} = 2g_{1313}\frac{\partial F}{\partial \sigma_{13}}\, dF\ .$$

Now

$$\frac{\partial F}{\partial \sigma_{22}} = \frac{\partial F}{\partial I_3}\ \tfrac{1}{2}(\sigma_{22}-\sigma_{33})$$

$$\frac{\partial F}{\partial \sigma_{33}} = -\frac{\partial F}{\partial I_3}\ \tfrac{1}{2}(\sigma_{22}-\sigma_{33}) \qquad (3.28)$$

$$\frac{\partial F}{\partial \sigma_{23}} = 2\frac{\partial F}{\partial I_3}\ \sigma_{23}$$

$$\frac{\partial F}{\partial \sigma_{12}} = 2\frac{\partial F}{\partial I_4}\ \sigma_{12}$$

$$\frac{\partial F}{\partial \sigma_{13}} = 2\frac{\partial F}{\partial I_4}\ \sigma_{13}\ .$$

Introducing (3.28) into (3.27) we have

$$
\begin{aligned}
d\varepsilon''_{11} &= 0 \\
d\varepsilon''_{22} &= (g_{2222}-g_{2233}) \frac{\partial F}{\partial I_3} \tfrac{1}{2}(\sigma_{22}-\sigma_{33})\, dF \\
d\varepsilon''_{33} &= -(g_{3322}-g_{3333}) \frac{\partial F}{\partial I_3} \tfrac{1}{2}(\sigma_{22}-\sigma_{33})\, dF \\
d\varepsilon''_{23} &= 2g_{2323} \frac{\partial F}{\partial I_3} 2\sigma_{23}\, dF \\
d\varepsilon''_{12} &= 2g_{1212} \frac{\partial F}{\partial I_4} 2\sigma_{12}\, dF \\
d\varepsilon''_{13} &= 2g_{1313} \frac{\partial F}{\partial I_4} 2\sigma_{13}\, dF .
\end{aligned}
\tag{3.29}
$$

Denote

$$
g_{2222} - g_{2233} = 2g_T . \tag{3.30}
$$

Since by (3.14) $d\varepsilon''_{22} = - d\varepsilon''_{33}$ it follows that

$$
d\varepsilon''_{22} = - d\varepsilon''_{33} = 2g_T \frac{\partial F}{\partial I_3} \tfrac{1}{2}(\sigma_{22}-\sigma_{33})\, dF .
$$

This result can be applied to the case $\sigma_{22} = -\sigma_{33}$ which produces a pure shear in a system of axes rotated at 45°. Because of transverse isotropy, the transverse shear stress-strain relation for $d\varepsilon''_{23}$ must apply to this case.

This procedure easily determines the stress-strain relation for $d\varepsilon''_{23}$. Thus we have

$$d\varepsilon''_{22} = 2g_T \frac{\partial F}{\partial I_3} \tfrac{1}{2}(\sigma_{22}-\sigma_{33})\, dF$$

$$d\varepsilon''_{33} = -\, 2g_T \frac{\partial F}{\partial I_3} \tfrac{1}{2}(\sigma_{22}-\sigma_{33})\, dF \qquad (3.31)$$

$$d\varepsilon''_{23} = 2g_T \frac{\partial F}{\partial I_3} \sigma_{23}\, dF$$

Denoting

$$2g_{1212} = g_A$$

it follows from transverse isotropy that

$$d\varepsilon''_{12} = 2g_A \frac{\partial F}{\partial I_4} \sigma_{12}\, dF$$

$$d\varepsilon''_{13} = 2g_A \frac{\partial F}{\partial I_4} \sigma_{13}\, dF \qquad (3.32)$$

The plastic work increment dW_p is given by

$$dW_p = \sigma_{ij} d\varepsilon''_{ij} \qquad (3.33)$$

Inserting (3.31-32) into this expression, we find

$$dW_p = 4\left(g_T \frac{\partial F}{\partial I_3} I_3 + g_A \frac{\partial F}{\partial I_4}\right) dF \qquad (3.34)$$

Because of the transverse isotropy dW_p can depend on stress only through the invariants of the stress tensor. It follows that

$$g_T = g_T\ (I_3,\ I_4)$$
$$g_A = g_A\ (I_3,\ I_4) \qquad (3.35)$$

To obtain information about the functions g_T and g_A, we shall use one dimensional stress-strain relations in transverse and axial shear. It will be recalled that a similar approach is useful in isotropic plasticity for isotropic J_2 theory. In that case, however, there is a single function g which is assumed to depend only on the single invariant J_2. The functional dependence $g(J_2)$ is then easily determined in terms of a single stress-strain relation e.g. uniaxial stress or pure shear. Another variant of this approach is in terms of a relation between so called effective stress and strain rate which are essentially square roots of J_2 of stress and strain rate.

Hill (ref. 17) has attempted to extend these concepts to orthotropic plasticity (see also further discussion in reference 18). However, unlike the isotropic case, the validity or even the existence of a relation between such defined effective stress and strain rate is not evident, as has also been pointed out by Hill. Here we have to bring in the anisotropy by two different functions g_T and g_A or in general by a tensorial g_{ijmn}. It should be noted, however, that with such a description it is not evident that Drucker's postulate will be universally satisfied.

Returning to the problem under consideration, let the principal shear stress for the plane stress system σ_{22}, σ_{33}, σ_{13} be denoted p_T and the principal shear stress for the stresses σ_{12}, σ_{13} be denoted p_A. It is seen from (3.20) that

$$I_3^{\sigma} = p_T^2 \qquad \text{(a)}$$

$$I_4^{\sigma} = p_A^2 \qquad \text{(b)} \tag{3.36}$$

where superscript σ denotes stress invariant. We may define similar invariants of plastic strain increment. Thus

$$I_3^{d\varepsilon''} = \tfrac{1}{4}(d\varepsilon''_{22} - d\varepsilon''_{33})^2 + (d\varepsilon''_{23})^2 = (\tfrac{1}{2}d\gamma''_T)^2$$

$$I_4^{d\varepsilon''} = (d\varepsilon''_{12})^2 + (d\varepsilon''_{13})^2 = (\tfrac{1}{2}d\gamma''_A)^2 \tag{3.37}$$

where the extreme right sides are squares of principal plastic shear strain rates.

The angle $\theta_{T\tau}$ between p_T and the x_2 axis is given by

$$\tan 2\theta_{T\tau} = -\frac{\sigma_{22} - \sigma_{33}}{2\sigma_{23}} \tag{3.38}$$

while the angle $\theta_{T\gamma}$ between $d\gamma''_T$ and the x_2 axis is given by

$$\tan 2\theta_{T\gamma} = -\frac{d\varepsilon''_{22} - d\varepsilon''_{33}}{2d\varepsilon''_{23}} \tag{3.39}$$

It is seen from (3.31) that these angles are the same. Therefore, the directions of p_T and $\frac{1}{2}d\gamma''_T$ coincide. The same conclusion is reached in similar fashion for the directions of p_A and $\frac{1}{2}d\gamma''_A$.

Introducing (3.31) into (3.37) yields the relations

$$d\gamma''_T = 2g_T \frac{\partial F}{\partial I_3} p_T \, dF$$

$$d\gamma''_A = 2g_A \frac{\partial F}{\partial I_4} p_A \, dF \tag{3.40}$$

With choice of the yield function (3.22) these relations assume the form

$$d\gamma_T'' = \frac{2g_T}{\tau_T^2} p_T \, dF \qquad \text{(a)}$$

$$d\gamma_A'' = \frac{2g_A}{\tau_A^2} p_A \, dF \, . \qquad \text{(b)} \qquad (3.41)$$

Consider the case of isothermal transverse principal shear p_T in the absence of axial shear. The one dimensional stress-strain relation may be written in the Ramberg-Osgood form

$$\gamma_T = \frac{p_T}{G_T} \left[1 + \left(\frac{p_T}{s_T}\right)^{m-1}\right] \qquad (3.42)$$

where G_T is the transverse shear modulus and s_T and m are curve fitting parameters. Because of the transverse isotropy this is the same as the stress-strain relation for σ_{23} and ε_{23}. It follows from (3.42) that

$$\gamma_T'' = \frac{p_T^m}{G_T s_T^{m-1}} \qquad \text{(a)}$$

$$d\gamma_T'' = \frac{m p_T^{m-1}}{G_T s_T^{m-1}} \, dp_T \qquad (3.43)$$

Also in the present case

$$F = \frac{I_3}{\tau_T^2} = \frac{p_T^2}{\tau_T^2} = 1 \qquad (3.44)$$

Introducing (3.43b-44) into (3.41a) we have

$$g_T(I_3,0) = \frac{m\tau_T^4}{8G_T s_T^{m-1}} p_T^{m-3}$$

Therefore, in view of (3.36a)

$$g_T(I_3,0) = \frac{m\tau_T^4}{8G_T s_T^{m-1}} I_3^{\frac{m-3}{2}} \quad . \tag{3.45}$$

The last equation follows from (3.25a) with $I_4 = 0$.

We now proceed in similar fashion for the case of isothermal axial principal shear in the absence of transverse shear. The Ramberg-Osgood presentation for one dimensional axial shear is

$$\gamma_A = \frac{p_A}{G_A} [1 + (\frac{p_A}{s_A})^{n-1}] \tag{3.46}$$

where G_A is axial shear modulus and s_A and n are curve fitting parameters. Because of the transverse isotropy this is the same as the stress-strain relation for σ_{12} and ε_{12}. We then obtain by the same procedure as before

$$g_A(0, I_4) = \frac{n\tau_A^4}{8G_A s_A^{n-1}} I_4^{\frac{n-3}{2}} \quad . \tag{3.47}$$

The last equation follows from (3.25b) with $I_3 = 0$.

The functions (3.45) and (3.47) define the isotropic hardening plastic strain rates for plane stress and for general axial shear but not for a combination of the two. In the first case, from (3.31), (3.22) and (3.45)

$$d\varepsilon''_{22} = \frac{m}{4G_T}\left(\frac{I_3}{s_T^2}\right)^{\frac{m-1}{2}} \tfrac{1}{2}(\sigma_{22}-\sigma_{33})\, dF$$

$$d\varepsilon''_{33} = -\frac{m}{4G_T}\left(\frac{I_3}{s_T^2}\right)^{\frac{m-1}{2}} \tfrac{1}{2}(\sigma_{22}-\sigma_{33})\, dF \qquad (3.48)$$

$$d\varepsilon''_{23} = \frac{m}{4G_T}\left(\frac{I_3}{s_T^2}\right)^{\frac{m-1}{2}} \sigma_{23}\, dF$$

In the second case, using (3.32), (3.22) and (3.47)

$$d\varepsilon''_{12} = \frac{n}{4G_A}\left(\frac{I_4}{s_A^2}\right)^{\frac{n-1}{2}} \sigma_{12}\, dF$$

$$d\varepsilon''_{13} = \frac{n}{4G_A}\left(\frac{I_4}{s_A^2}\right)^{\frac{n-1}{2}} \sigma_{13}\, dF \qquad (3.49)$$

The preceding results are special cases. For an arbitrary state of stress g_T and g_A are functions of I_3 and I_4, (3.35). In attempting to construct such functions we shall require that in the special cases discussed above these functions reduce to (3.45) and (3.47). Furthermore, stress-strain relations established must include isotropic J_2 theory as a special case when the material becomes isotropic in shear. This will be the case when

$$s_T = s_A \qquad \tau_{To} = \tau_{Ao}$$

$$G_T = G_A \qquad n = m .$$

In this event

$$g_T = g_A$$

and J_2 is a linear function of I_3 and I_4. To comply with these requirements, a convenient, albeit non-unique, choice is to assume that

$$g_T = g_T \, (I_3/s_T^{\,2} + I_4/s_A^{\,2})$$

$$g_A = g_A \, (I_3/s_T^{\,2} + I_4/s_A^{\,2}) \; . \tag{3.50}$$

The only functions (3.50) which comply with (3.45) and (3.47) are

$$2g_T = \frac{m\tau_T^{\,4}}{4G_T s_T^{\,2}} \left(\frac{I_3}{s_T^{\,2}} + \frac{I_4}{s_A^{\,2}}\right)^{\frac{m-3}{2}}$$

$$2g_A = \frac{n\tau_A^{\,4}}{4G_A s_A^{\,2}} \left(\frac{I_3}{s_T^{\,2}} + \frac{I_4}{s_A^{\,2}}\right)^{\frac{n-3}{2}} . \tag{3.51}$$

Introducing these functions and the yield function (3.22) into (3.31-32) and taking into account (3.22) we have for the isothermal case

$$d\varepsilon''_{ij} = \frac{m\tau_{To}^2}{4G_T s_T^2} \left(I_3/s_T^2 + I_4/s_A^2\right)^{\frac{m-3}{2}} \left(dI_3/\tau_{To}^2 + dI_4/\tau_{Ao}^2\right) s_{ij} \qquad (3.52)$$

where

$i, j = 2, 3$

$s_{22} = \frac{1}{2}(\sigma_{22} - \sigma_{33}) = -s_{33} \qquad s_{23} = \sigma_{23}$

$$d\varepsilon''_{1i} = \frac{n\tau_{Ao}^2}{4G_A s_A^2} \left(I_3/s_T^2 + I_4/s_A^2\right)^{\frac{n-3}{2}} \left(dI_3/\tau_{To}^2 + dI_4/\tau_{Ao}^2\right) s_{1i} \qquad (3.53)$$

$s_{12} = \sigma_{12} \qquad s_{13} = \sigma_{13}$

Equations (3.52-53) define the incremental isothermal plastic stress-strain relations in terms of the initial yield stresses τ_{To} and τ_{Ao}, the Ramberg-Osgood parameters s_T, m, s_A and n and the elastic shear moduli G_T and G_A.

We shall now consider some special cases of interest.

1. Proportional Loading

This implies that all stresses grow in fixed ratios to one another. Thus

$$\sigma_{ij} = \zeta\sigma_{ij}(o)$$

$$d\sigma_{ij} = d\zeta\sigma_{ij}(o) \tag{3.54}$$

where $\sigma_{ij}(o)$ is some initial stress state. If (3.54) are introduced into (3.52-53) taking into account (3.20), the stress-strain relations can be integrated. The results are

$$\varepsilon''_{ij} = \frac{\tau_{To}^2}{4G_T s_T^2} \left(I_3/s_T^2 + I_4/s_A^2\right)^{\frac{m-3}{2}} \left(I_3/\tau_{To}^2 + I_4/\tau_{Ao}^2\right) s_{ij} \tag{a}$$

(3.55)

$$\varepsilon''_{li} = \frac{\tau_{Ao}^2}{4G_A s_A^2} \left(I_3/s_T^2 + I_4/s_A^2\right)^{\frac{n-3}{2}} \left(I_3/\tau_{To}^2 + I_4/\tau_{Ao}^2\right) s_{li} \tag{b}$$

$i,j = 2,3$

2. Plane Stress in the x_1x_2 Plane

This case is of importance for balanced symmetric laminates which consist of unidirectionally reinforced layers. For membrane type loading, i.e. force resultants in the mid-plane of the laminate and no bending moments, the state of stress

in any lamina is plane except for a boundary layer near the edges. The stress state on a typical lamina element is shown in figure 23. It follows from (3.20) that in the present case

$$I_3 = \tfrac{1}{4}\sigma_{22}^2 \qquad I_4 = \sigma_{12}^2$$

Then from (3.52-53)

$$d\varepsilon''_{22} = \frac{m\tau_{To}^2}{4G_T s_T^2}\left(\sigma_{22}^2/4s_T^2 + \sigma_{12}^2/s_A^2\right)^{\frac{m-3}{2}}$$

$$\sigma_{22}\left[\left(\sigma_{22}/4\tau_{To}^2\right) d\sigma_{22} + \left(\sigma_{12}/\tau_{Ao}^2\right) d\sigma_{12}\right] \qquad (3.56)$$

$$d\varepsilon''_{12} = \frac{n\tau_{Ao}^2}{4G_A s_A^2}\left(\sigma_{22}^2/4s_T^2 + \sigma_{12}^2/s_A^2\right)^{\frac{n-3}{2}}$$

$$\sigma_{12}\left[\left(\sigma_{22}/4\tau_{To}^2\right) d\sigma_{22} + \left(\sigma_{12}/\tau_{Ao}^2\right) d\sigma_{12}\right]$$

and

$$d\varepsilon''_{11} = 0$$

For the case of proportional loading these equations integrate into

$$\varepsilon''_{22} = \frac{\tau_{To}^2}{4G_T s_T^2} \left(\sigma_{22}^2/4s_T^2 + \sigma_{12}^2/s_A^2\right)^{\frac{m-3}{2}}$$

$$\left(\sigma_{22}^2/4\tau_{To}^2 + \sigma_{12}^2/\tau_{Ao}^2\right) \sigma_{22}$$

$$\varepsilon''_{12} = \frac{\tau_{Ao}^2}{4G_A s_A^2} \left(\sigma_{22}^2/4s_T^2 + \sigma_{12}^2/s_A^2\right)^{\frac{n-3}{2}} \qquad (3.57)$$

$$\left(\sigma_{22}^2/4\tau_{To}^2 + \sigma_{12}^2/\tau_{Ao}^2\right) \sigma_{12}$$

$$\varepsilon''_{11} = 0$$

Next we consider the loading paths shown in figure 24. The loading $\vec{OC}$ represents the proportional loading considered above. The other load paths represent uniaxial stress first and shear second, and vice versa. For the loading $\vec{OAC}$ equations (3.56) can be integrated to give the results

$$\varepsilon''_{22}\ (C) = \frac{\sigma_{22}}{4G_T} \left(\frac{\sigma_{22}}{2s_T}\right)^{m-1} + \left[\frac{1}{8G_T} \frac{m}{m-1} \left(\frac{\tau_{To}}{\tau_{Ao}}\right)\right.$$

$$\left.\left(\frac{s_A}{s_T}\right)^2 \left(\sigma_{22}^2/4s_T^2 + \sigma_{12}^2/s_A^2\right)^{\frac{m-1}{2}} - \left(\sigma_{22}^2/4s_T^2\right)^{\frac{m-1}{2}}\right] \sigma_{22}$$

$$\varepsilon''_{12}(C) = \frac{n}{4G_A s_A^2} \int_0^{\sigma_{12}} (\sigma_{22}^2/4s_T^2 + \sigma_{12}^2/s_A^2)^{\frac{n-3}{2}} \sigma_{12}^2 \, d\sigma_{12}$$

For the loading $O\vec{B}C$

$$\varepsilon''_{22}(C) = \frac{m}{16G_T s_T^2} \int_0^{\sigma_{22}} (\sigma_{22}^2/4s_T^2 + \sigma_{12}^2/s_A^2)^{\frac{m-3}{2}} \sigma_{22}^2 \, d\sigma_{22}$$

$$\varepsilon''_{12}(C) = \frac{\sigma_{12}}{2G_A} \left(\frac{\sigma_{12}}{A}\right)^{n-1} + \left\{\frac{n}{n-1} \frac{1}{4G_A} \left(\frac{\tau_{Ao}}{\tau_{To}}\right)^2 \right.$$
$$\left. [(\sigma_{22}^2/4s_T^2 + \sigma_{12}^2/s_A^2)^{\frac{n-1}{2}} - (\sigma_{12}^2/s_A^2)^{\frac{n-1}{2}}] \sigma_{12} \right\}$$

TEMPERATURE DEPENDENT STRESS-STRAIN RELATIONS

It is a well known fact that the yield stresses of materials decrease with rising temperature and, therefore, it is to be expected that yield surfaces will contract when the temperature increases. This implies that the same state of stress produces larger plastic strains for higher temperatures. Phillips, reference 19, has conducted extensive tests to determine the variation of the yield surfaces of metals with temperature. His results for aluminum indicate that the initial yield surface at any temperature is accurately described by a Mises ellipse and that the dimensions of the ellipse decrease linearly with rising temperature, figure 25. We are not aware of similar experiments for metal matrix composites and in the absence of such information we shall extend these findings to the present situation in generalized fashion. We shall assume that with temperature rise the yield surface shrinks in self similar fashion. This implies that all stress parameters defining the yield surface change in similar fashion with temperature. In particular, the quadratic initial yield function (3.23) may be considered as a yield function at a reference temperature ϕ_r and is accordingly written

$$I_3/\tau_{Tor}^2 + I_4/\tau_{Aor}^2 = 1 \tag{4.1}$$

Then the initial yield functions at some other temperature ϕ is

$$I_3/\tau_{To}^2(\phi) + I_4/\tau_{Ao}^2(\phi) = 1 \tag{4.2}$$

where temperature self similarity is expressed by

$$\begin{aligned} \tau_{To}(\phi) &= \tau_{Tor} f(\phi) \\ \tau_{Ao}(\phi) &= \tau_{Aor} f(\phi) \end{aligned} \tag{4.3}$$

If the yield stresses decrease linearly with temperature as in the experimental results shown in figure 26 and if the yield surface "shrinks to zero" at the same temperature ϕ_u, figure 26, then

$$f(\phi) = \frac{\phi_u - \phi}{\phi_u - \phi_r} \quad . \tag{4.4}$$

At any temperature ϕ it is assumed as in section 3 that the material hardens in transversely isotropic fashion. Therefore, the subsequent yield surfaces at temperature ϕ are again given by

$$I_3/\tau_T(\phi)^2 + I_4/\tau_A(\phi)^2 = 1 \tag{4.5}$$

where $\tau_T(\phi)$ and $\tau_A(\phi)$ are related to $\tau_{To}(\phi)$ and $\tau_{Ao}(\phi)$ by (3.25). We can also express the temperature dependence of the initial yield surface in the form

$$\frac{I_3}{\tau_{Tor}^2} + \frac{I_4}{\tau_{Aor}^2} - f^2(\phi) = 0 \quad . \tag{4.6}$$

Similarly, the temperature dependence of subsequent yield surfaces may be given by

$$\frac{I_3}{\tau_{Tr}^2} + \frac{I_4}{\tau_{Ar}^2} - f^2(\phi) = 0 \tag{4.7}$$

where τ_{Tr} and τ_{Ar} are the parameters of subsequent yield surfaces at the reference temperature ϕ_r. The relations between τ_{Tr}, τ_{Ar} and τ_T, τ_A is given by (4.3). Thus

$$\begin{aligned} \tau_T(\phi) &= \tau_{Tr} f(\phi) \\ \tau_A(\phi) &+ \tau_{Ar} f(\phi) \quad . \end{aligned} \tag{4.8}$$

In regard to the functions g_T and g_A we can follow through the method of their construction, discussed in the previous section, at any temperature ϕ with Ramberg-Osgood parameters for that temperature. Thus, if the shear stress-strain relations at temperature ϕ are expressed as

$$\varepsilon_{23} = \frac{\sigma_{23}}{2G_T(\phi)} \left\{ 1 + \left[\frac{\sigma_{23}}{s_T(\phi)} \right]^{m(\phi)-1} \right\}$$

$$\varepsilon_{12} = \frac{\sigma_{12}}{2G_A(\phi)} \left\{ 1 + \left[\frac{\sigma_{12}}{s_A(\phi)} \right]^{n(\phi)-1} \right\} \tag{4.9}$$

then in analogy to (3.51)

$$2g_T = \frac{\tau_T(\phi)^4}{4G_T(\phi)\, s_T(\phi)^2} \left[\frac{I_3}{s_T(\phi)^2} + \frac{I_4}{s_A(\phi)^2} \right]^{\frac{1}{2}[m(\phi)-3]}$$

$$2g_A = \frac{n(\phi)\tau_A(\phi)^4}{4G_A(\phi)\, s_A(\phi)^2} \left[\frac{I_3}{s_T(\phi)^2} + \frac{I_4}{s_A(\phi)^2} \right]^{\frac{1}{2}[n(\phi)-3]} \tag{4.10}$$

The stress-strain relations are now

$$\begin{aligned} d\varepsilon_{11} &= d\varepsilon'_{11} + \alpha_A d\phi \\ d\varepsilon_{ij} &= d\varepsilon'_{ij} + 2g_T \frac{\partial F}{\partial I_3} s_{ij} dF + \alpha_T \delta_{ij} d\phi \\ d\varepsilon_{1i} &= d\varepsilon'_{1i} + 2g_A \frac{\partial F}{\partial I_4} s_{1i} dF \end{aligned} \tag{4.11}$$

$i, j = 2, 3$

where the elastic strain increments are given by (3.6), α_A and α_T are axial and transverse temperature dependent tangent thermal expansion coefficients, δ_{ij} is the Kronecker delta and

$$[s_{ij}] = \begin{bmatrix} 0 & \sigma_{12} & \sigma_{13} \\ \sigma_{12} & \tfrac{1}{2}(\sigma_{22}-\sigma_{33}) & \sigma_{23} \\ \sigma_{13} & \sigma_{23} & -\tfrac{1}{2}(\sigma_{22}-\sigma_{33}) \end{bmatrix} .$$

The increment dF is given by

$$dF = \frac{\partial F}{\partial I_3}\, dI_3 + \frac{\partial F}{\partial I_4}\, dI_4 + \frac{\partial F}{\partial \phi}\, d\phi$$

using the yield function F = 0. Applying this to (4.5) and using (4.8) we find

$$dF = \frac{dI_3}{\tau_T(\phi)^2} + \frac{dI_4}{\tau_A(\phi)^2} - \frac{2f'(\phi)}{f(\phi)}\, d\phi \cdot \qquad (4.12)$$

The temperature dependent plastic strains in (4.11) can now be written explicitly as follows

$$d\varepsilon''_{ij} = \frac{m\tau_{Tor}^2}{4G_T r_T^2} (I_3/s_T^2 + I_4/s_A^2)^{\frac{m-3}{2}} [dI_3/\tau_{Tor}^2 + dI_4/\tau_{Aor}^2 - 2\tau_{Tor}^2 (I_3/\tau_{Tor}^2 + I_4/\tau_{Aor}^2)\frac{f'(\phi)}{f(\phi)}\, d\phi]s_{ij} \qquad (4.13)$$

$$d\varepsilon''_{1i} = \frac{n\tau_{Aor}^{2}}{4G_A s_A^{2}} \left(I_3/s_T^{2} + I_4/s_A^{2}\right)^{\frac{n-3}{2}} \left[dI_3/\tau_{Tor}^{2} + dI_4/\tau_{Aor}^{2} - 2\tau_{Aor}^{2}\right.$$

$$\left.\left(I_3/\tau_{Tor}^{2} + I_4/\tau_{Aor}^{2}\right) \frac{f'(\phi)}{f(\phi)}\, d\phi\right] s_{1i} \qquad (4.14)$$

$i, j = 2,3$

where we have used (3.25) and (4.3), and all material parameters in (4.17-18) are functions of temperature.

We consider some special cases of (4.13-14).

1. Heating at constant stress

In this event

$$d\varepsilon''_{ij} = -\frac{m\tau_{Tor}^{4}}{2G_T s_T^{2}} \left(I_3/s_T^{2} + I_4/s_A^{2}\right)^{\frac{m-3}{2}} \left(I_3/\tau_{Tor}^{2} + I_4/\tau_{Aor}^{2}\right) \frac{f'(\phi)}{f(\phi)}\, s_{ij}\, d\phi$$

$$d\varepsilon''_{1i} = -\frac{n\tau_{Aor}^{4}}{2G_A s_A^{2}} \left(I_3/s_T^{2} + I_4/s_A^{2}\right)^{\frac{n-3}{2}} \left(I_3/\tau_{Tor}^{2} + I_4/\tau_{Aor}^{2}\right) \frac{f'(\phi)}{f(\phi)}\, s_{1i}\, d(\phi). \qquad (4.15)$$

When the temperature is changed from ϕ_r to ϕ the strains at ϕ are given by

$$\varepsilon''_{ij}(\phi) = \varepsilon''_{ij}(\phi_r) + \int_{\phi_r}^{\phi} \frac{d\varepsilon''_{ij}}{d\phi}\, d\phi$$

$$\varepsilon''_{1i}(\phi) = \varepsilon''_{1i}(\phi_r) + \int_{\phi_r}^{\phi} \frac{d\varepsilon''_{1i}}{d\phi}\, d\phi \ . \qquad (4.16)$$

These integrals can be carried out if the temperature dependence of all physical parameters in (4.9) is known. In order to determine such temperature dependence, it is necessary to have a set of transverse and axial shear stress-strain relations at various temperatures and to model each by the representation (4.9). Such stress-strain relations can be obtained experimentally or numerically. Here we have chosen the second alternative. The stress-strain relations at various temperatures have been obtained by the methods described previously with the help of the ANSYS computer code, based on matrix property changes with temperature. Such results were shown for transverse shear in figure 20 and for axial shear in figure 22. Each of the stress-strain relations was fitted into a Ramberg-Osgood form (4.9) and the resulting parameters s_T, s_A, m and n were plotted as functions of temperature. Such plots are shown in figures 27-30. The initial yield stresses τ_{To} and τ_{Ao} were determined from each stress-strain curve as the points where the linear relation ended. Plots of these as functions of temperature are shown in figures 31-32.

All of the stress-strain relations are based on the premise that the composite has no internal stresses at room temperature (RT). This, however, is not necessarily realistic since a metal matrix composite is manufactured at elevated temperature at which, it may be assumed, there are no significant internal stresses. As the composite is cooled down to RT, significant internal stresses develop, tensile in the matrix and compressive in the fibers. If the composite is now loaded in shear, the residual matrix stresses interact with matrix stresses due to load and, therefore, the stress-strain relation will be different from that for specimens with no residual stresses at RT. Note that the linear part of the stress-strain relation is not changed by the residual stresses.

To illustrate these phenomena, we have performed numerical analyses of the hexagonal array model. The composite has been assumed stress-free at 371°C. The internal stresses due to cool-down to RT have been determined. After that, two subsequent

analyses were performed. In the first, a transverse shear loading was applied. In the second, the composite was re-heated to 260°C and then the shear loading applied. Both these analyses were shown in figure 21 and compared with analyses where the material was presumed stress-free at room temperature and 260°C. These curves demonstrate that the plastic strains are much larger when residual stresses are included. In both analyses where residual stresses were included, the elastic portion of the response was severely limited in extent. The initial moduli were identical to the solution without processing stresses, however.

Similar phenomena can be expected for axial shear but we have not performed the numerical analysis for this case.

These findings are of significance for the general stress-strain relations as developed in this work. The point of view taken here is that the basic information entering into the stress-strain relations is transverse and axial shear stress-strain relations as a function of temperature. If the three dimensional stress-strain relations are required for a composite which has residual stresses due to cool-down, then it is necessary to use the temperature dependent parameters of shear stress-strain relations with residual stress in the same fashion as done above.

This completes the discussion of the three dimensional temperature dependent stress-strain relations. It is, of course, necessary to examine the validity of the stress-strain relations and this can be done experimentally or numerically. In the latter case, it is necessary to compute stress-strain relations under some states of combined stress by the incremental methods developed in the section METHODS OF ANALYSIS and to compute the same stress-strain relations on the basis of the theory developed in subsequent chapters, based on numerically obtained one dimensional stress-strain relations, examining whether the two sets of stress-strain relations are close. Unfortunately, the scope of the present contract did not permit such an examination since the computer time needed is quite extensive. The ANSYS computer code, which we have judged most suitable for our purposes, is very expensive to run for such cases.

CONCLUSION

We have established a general method of analysis for incremental loading and heating of metal matrix composites modelled by a periodic hexagonal array of identical circular fibers. The matrix is temperature dependent isotropic elasto-plastic and the fibers are temperature dependent transversely isotropic elastic. The analysis must be carried out numerically but it has been shown that it is sufficient to analyze one two dimensional repeating element for generalized plane strain and for antiplane strain. Utilizing this method, we have obtained a variety of one dimensional effective stress-strain relations at various temperatures and for various temperature histories. Thermal expansion characteristics without and with external load have also been determined. In all numerical analyses we have employed the ANSYS code.

Next we have established a general set of incremental temperature dependent elasto-plastic stress-strain relations for the fiber composite based on transverse isotropy of the composite and the assumption of transversely isotropic hardening. A unique feature of the stress-strain relations is that the only information required is one dimensional temperature dependent stress-strain relations in transverse and axial shear. Such stress-strain relations we have obtained numerically but it is equally possible to utilize experimentally obtained stress-strain relations.

It seems that the most problematic assumption in this work is transversely isotropic hardening of the composite which implies that the yield surface changes in self similar fashion in stress-temperature space. It is believed that such an assumption is sufficiently accurate for initial loading of a metal matrix fiber composite but not necessarily for repeated loadings. Experience with metals shows that for such loadings the yield surface for subsequent loadings deforms and translates in stress space and it is possible that similar phenomena will occur for metal matrix composites.

Another idealization which is used for metals is kinematic hardening which assumes that the yield surface translates in stress space without changing its form. This, however, cannot be compatible with temperature dependence for the yield surface must shrink with increasing temperature and, thus, temperature history cannot be accommodated within pure kinematic hardening. Thus, idealized as the assumption of transversely isotropic hardening may be, it is difficult to see a viable alternative to it.

The validity of the stress-strain proposed must, of course, be examined and this should preferably be done by experiment.

REFERENCES

1. Hill, R., "The Essential Structure of Constitutive Laws for Metal Composites and Polycrystals," J. Mech. Phys. Solids, 15, 79 (1967).
2. Hashin, Z., in NASA CR-207 (1965).
3. Shu, L.S. and Rosen, B.W., "Strength of Fiber Reinforced Composites by Limit Analysis Methods," J. Composite Materials, 1, 366 (1967).
4. Adams, D.F., "Inelastic Analysis of a Unidirectional Composite Subjected to Transverse Normal Loading," J. Composite Materials, 4, 310 (1970).
5. Foye, R.L., "Theoretic Post Yielding Behavior of Composite Laminates, Part I - Inelastic Micromechanics," J. Composite Materials, 7, 178 (1973).
6. Lin, T.H., Salinas, D., and Ito, Y.M., "Elastic Plastic Analysis of Unidirectional Composites," J. Composite Materials, 6, 48 (1972).
7. Huang, W.C., "Plastic Behavior of Some Composite Materials," J. Composite Materials, 5, 320 (1971).
8. Huang, W.C., "Elastoplastic Transverse Properties of a Unidirectional Fibre Reinforced Composite," J. Composite Materials, 7, 482 (1973).
9. Dvorak, G.J., Rao, M.S.M., and Tarn, J.Q., "Yielding in Unidirectional Composites under External Loads and Temperature Changes," J. Composite Materials, 7 , 94 (1973).
10. Dvorak, G.J., Rao, M.S.M., and Tarn, J.Q., "Generalized Initial Yield Surfaces for Unidirectional Composites," J. Appl. Mech., 41, 249 (1974).
11. Dvorak, G.J. and Rao, M.S.M., "Axisymmetric Plasticity Theory of Fibrous Composites," Int. J. Engrg. Sci., 14. 361 (1976).
12. Dvorak, G.J. and Bahei-el-Din, Y.A., "Elastic-Plastic Behavior of Fibrous Composites," J. Mech. Phys. Solids, 27, 51 (1979).

13. Mulhern, J.F., Rogers, T.G. and Spencer, A.J.M., "A Continuum Model for Fiber-Reinforced Plastic Materials," Proc. Roy. Soc., A 301, 473 (1967).
14. Hashin, Z., "Theory of Fiber Reinforced Materials," NASA CR 1974 (1972).
15. Hashin, Z. and Rosen, B.W., "The Elastic Moduli of Fiber Reinforced Materials," J. Appl. Mech., 31, 233 (1964).
16. Kohnke, P., "ANSYS Engineering Analysis System Theoretical Manual," Swanson Analysis Systems, Inc. (1977).
17. Hill, R., Plasticity, Chapter XII, Oxford (1950).
18. Hill, R., "Theoretical Plasticity of Textured Aggregates," Math-Proc. Cambridge Phil. Soc. 85, 179 (1979).
19. A. Phillips, "The Foundations of Thermoplasticity-Experiments and Theory" in Topics in Applied Continuum Mechanics, J.L. Zeman and F. Ziegler, Eds., p.1, Springer Verl. (1974).

Table 1. Elastic Constants (Room Temperature)

Elastic Constant	T-50 Graphite Fiber	2024-T4 Al Matrix
E_A (GPa)	388.2	72.4
E_T (GPa)	7.6	72.4
G_{AT} (GPa)	14.9	27.2
G_{TT} (GPa)	2.6	27.2
ν_{AT}	0.41	0.33
ν_{TT}	0.45	0.33
α_A m/m/°C	-0.68×10^{-6}	22.5×10^{-6}
α_T m/m/°C	9.74×10^{-6}	22.5×10^{-6}

A = Axial (Longitudinal)

T = Transverse

Table 2. Elastic Results (Room Temperature)

Elastic Constant	CCA*	F.E.**	% Difference
E_T (GPa)	41.78	42.26	1.1
G_{TT} (GPa)	14.99	15.13	0.9
G_A (GPa)	22.87	23.20	1.6
ν_{TT}	0.394	0.396	0.5
ν_{AT}	0.338	0.340 +	0.6
α_A m/m/°C	6.36	6.36	0.0
α_T m/m/°C	25.65	25.69	0.2

A = Axial (Longitudinal)

T = Transverse

*Composite Cylinder Assemblage

**Finite Element

+Computed using E_A from Rule of Mixtures and F.E. Results

Table 3. Transverse Tension and Temperature, Isotropic Hardening

Load Path	ε_2 %	ε_3 %	ε_1 %
1-2-3	-0.205	-0.616	-0.074
1-4	-0.190	-0.619	-0.073
% Difference	7.6	0.5	1.4
1-5-6	0.373	-0.506	-0.010
1-7	0.336	-0.465	-0.030
% Difference	10.4	8.4	NA

Load Steps

1. Stress Free Temperature to Room Temperature
2. Room Temperature to 204°C
3. σ_2 - 0 to 113.8 MPa
4. Simultaneous σ_2 - 0 to 113.8 and Room Temperature to 204°C
5. σ_2 - 0 to 172.4 MPa
6. Room Temperature to 299°C
7. Simultaneous σ_2 - 0 to 172.4 MPa and Room Temperature to 299°C

Table 4. Transverse Compression and Temperature, Isotropic Hardening

Load Path	ε_2 %	ε_3 %	ε_1 %
1-2-3	-0.790	-0.382	0.008
1-4	-0.794	-0.371	-0.018
% Difference	0.5	2.9	NA

Load Steps

1. Stress Free Temperature to Room Temperature
2. Room Temperature to 204°C
3. σ_2 - 0 to -113.8 MPa
4. Simultaneous σ_2 - 0 to -113.8 and Room Temperature to 204°C

Table 5. Transverse Tension and Temperature, Kinematic Hardening

Load Path	ε_2 %	ε_3 %	ε_1 %
1-2-3	-0.201	-0.614	-0.079
1-4	-0.234	-0.616	-0.077
% Difference	15.2	0.3	2.6

Load Steps

1. Stress Free Temperature to Room Temperature
2. Room Temperature to 204°C
3. σ_2 - 0 to 113.8 MPa
4. Simultaneous σ_2 - 0 to 113.8 and Room Temperature to 204°C

Table 6. σ_2 and σ_3, Isotropic Hardening

Load Path	ε_2 %	ε_3 %	ε_1 %
1-2	0.698	-0.579	-0.0214
2-4	0.693	-0.580	-0.0197
3	0.696	-0.581	-0.0203
Max % Difference	0.7%	0.3%	7.9%

Lead Steps

1. σ_2 - 0 to 180 MPa
2. σ_3 - 0 to -90 MPa
3. Simultaneous σ_2 - 0 to 180 MPa and σ_3 - 0 to -90 MPa

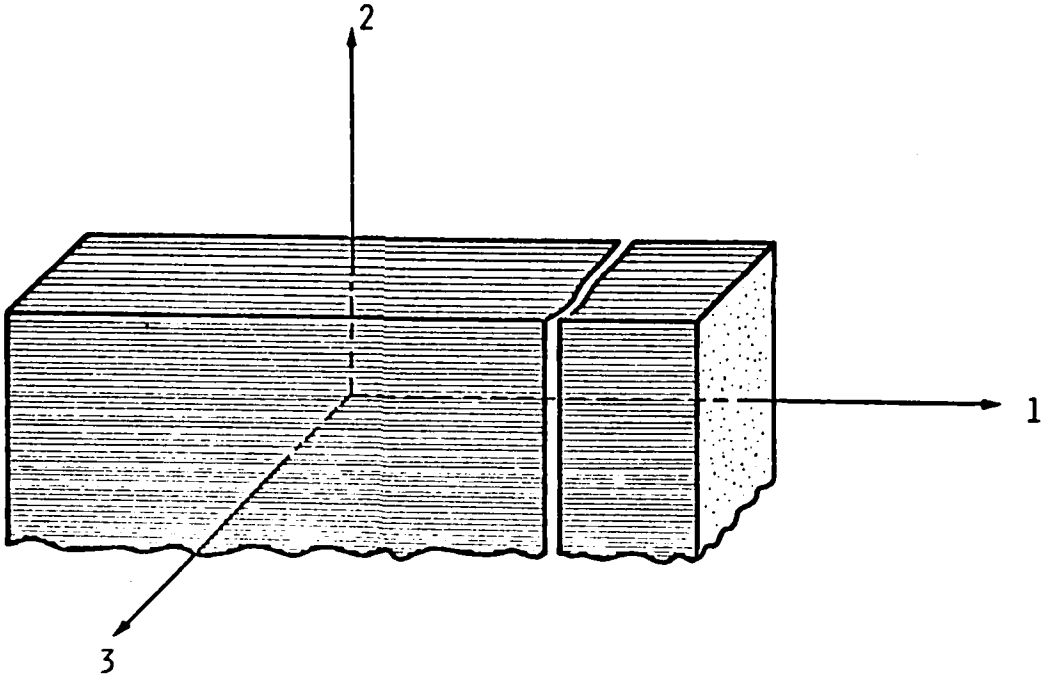

Figure 1. Unidirectionally Reinforced Lamina

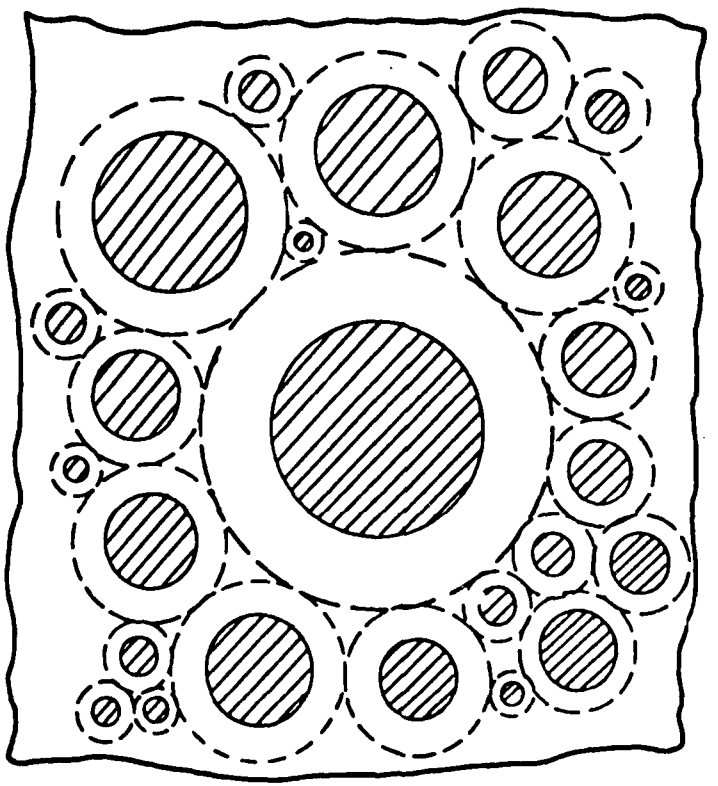

Figure 2. Composite Cylinder Assemblage-Construction

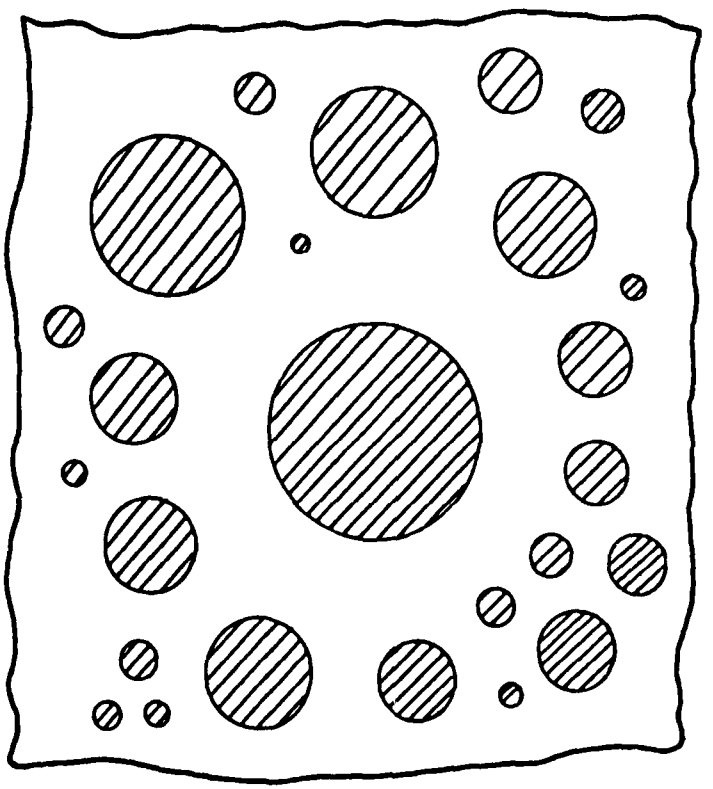

Figure 3. Composite Cylinder Assemblage

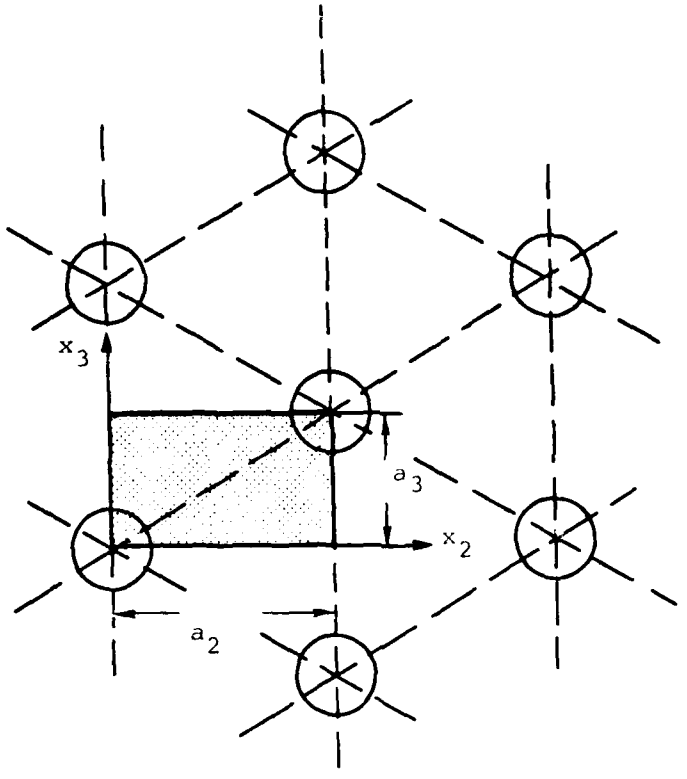

Figure 4. Hexagonal Fiber Array and Typical Repeating Element

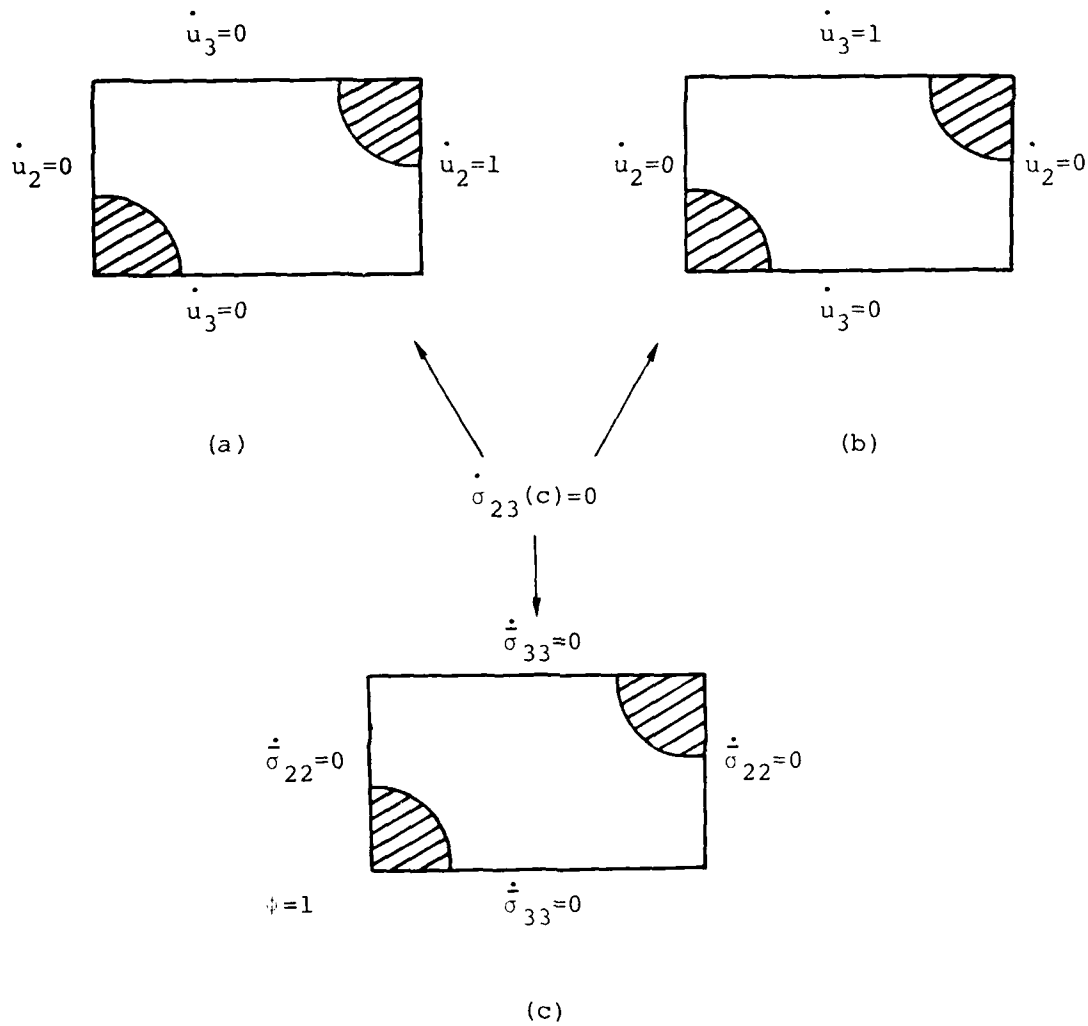

Figure 5. Boundary Value Problems

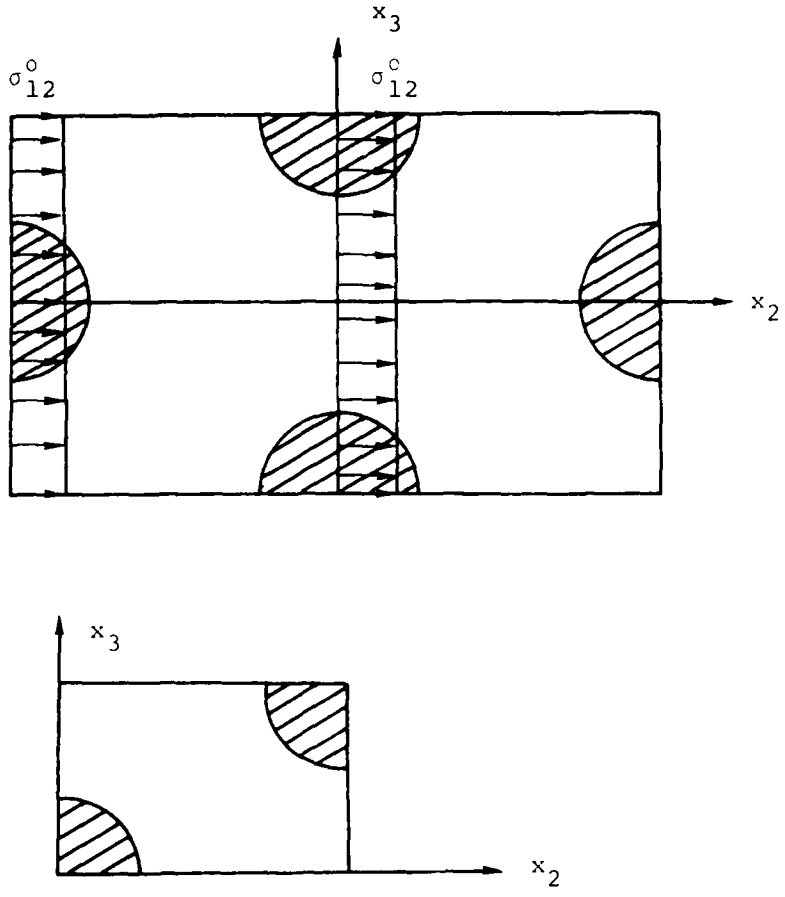

Figure 6. Axial Shear Symmetries

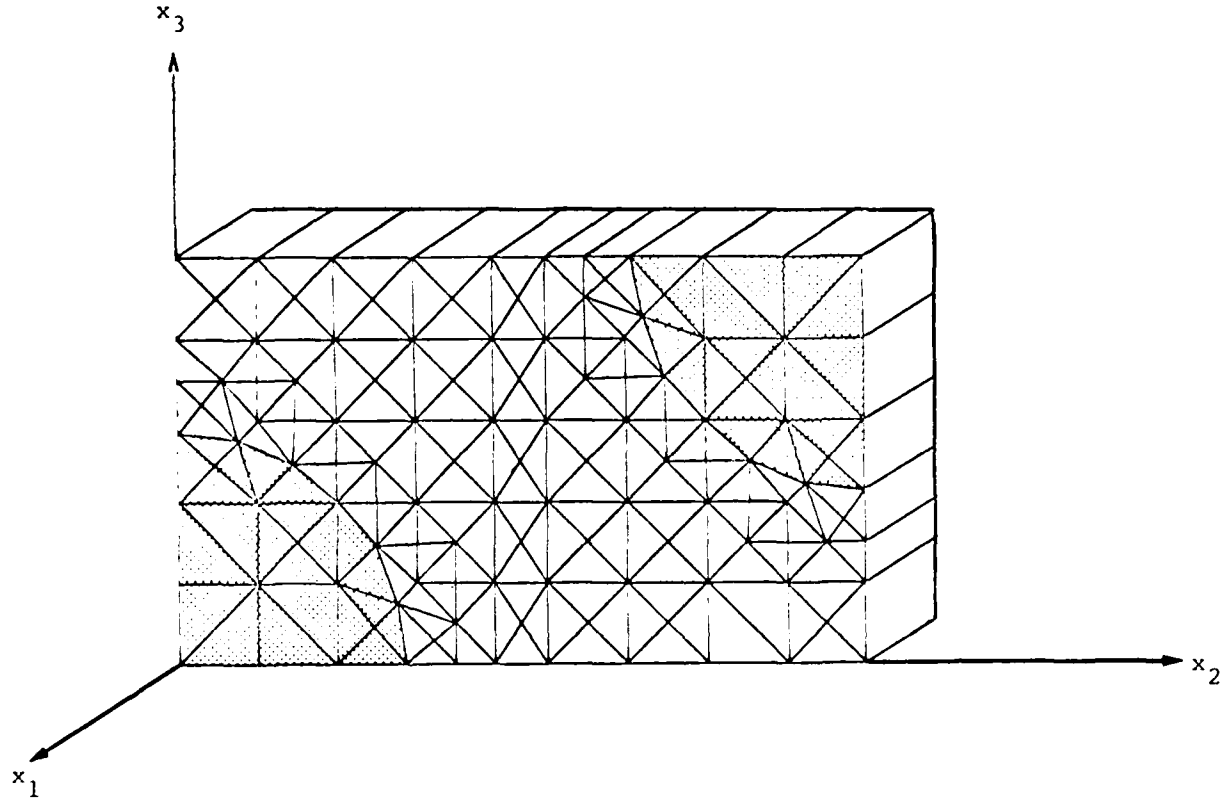

Figure 7. Finite Element Model

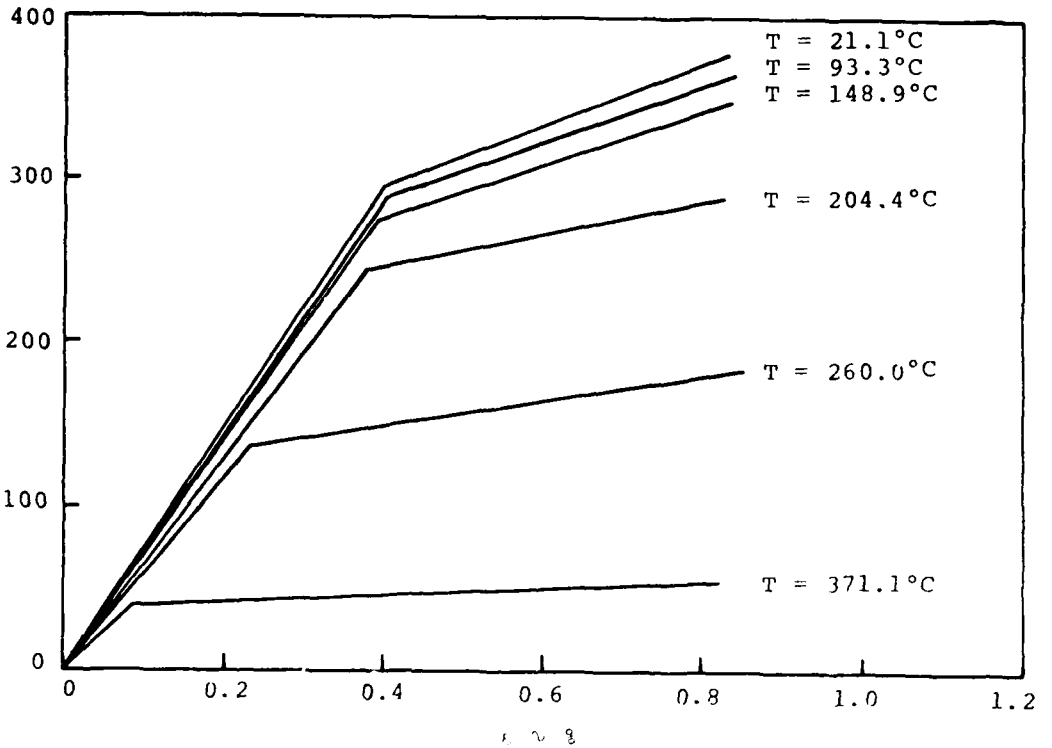

Figure 8. Input Matrix Properties, Kinematic Hardening

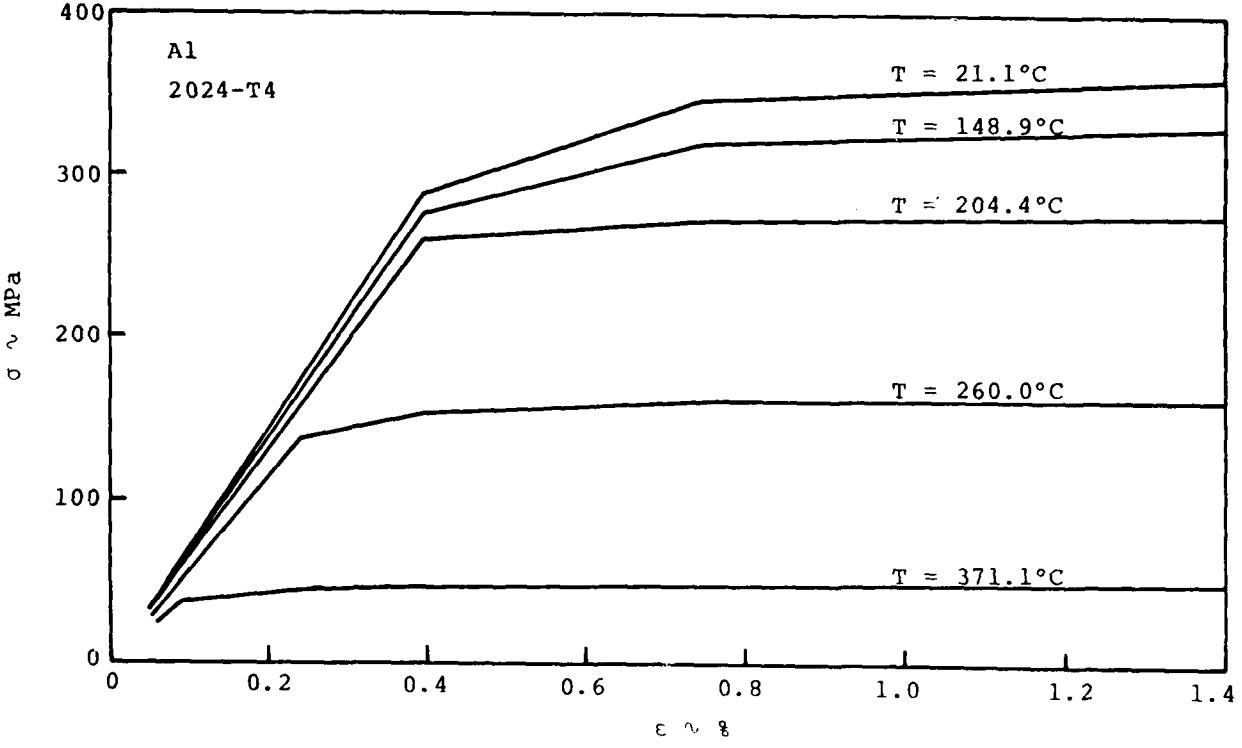

Figure 9. Input Matrix Properties, Isotropic Hardening

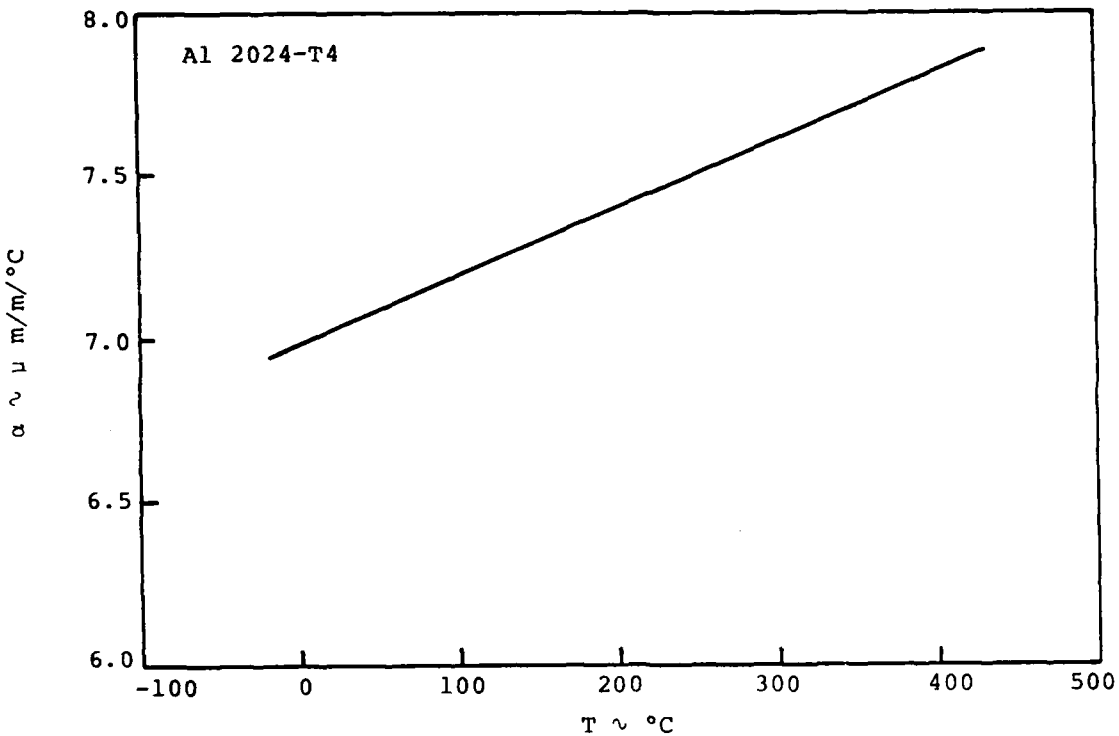

Figure 10. Coefficient of Thermal Expansion vs. Temperature of Aluminum Matrix

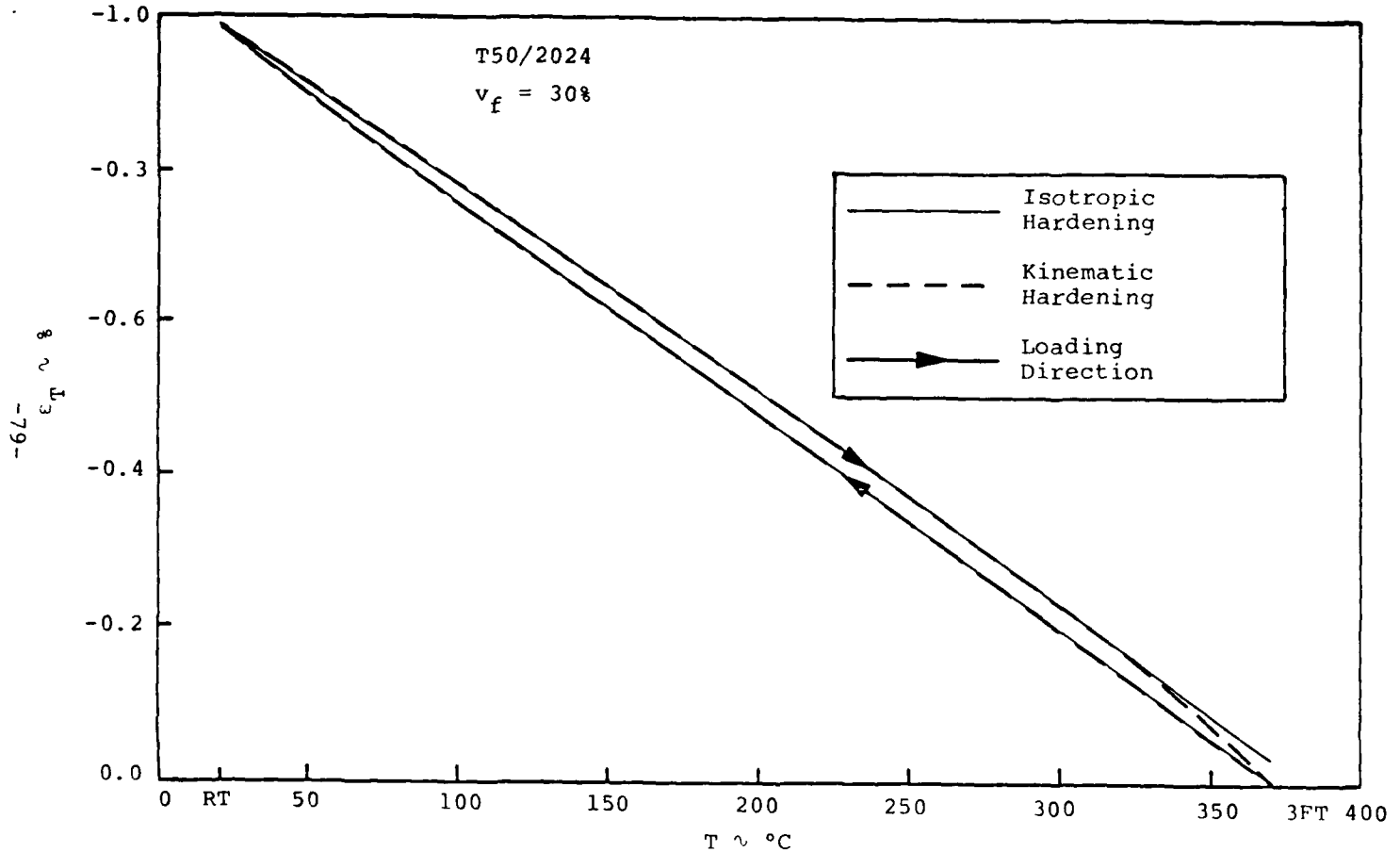

Figure 11. Transverse Thermal Expansion, Isotropic vs. Kinematic Hardening

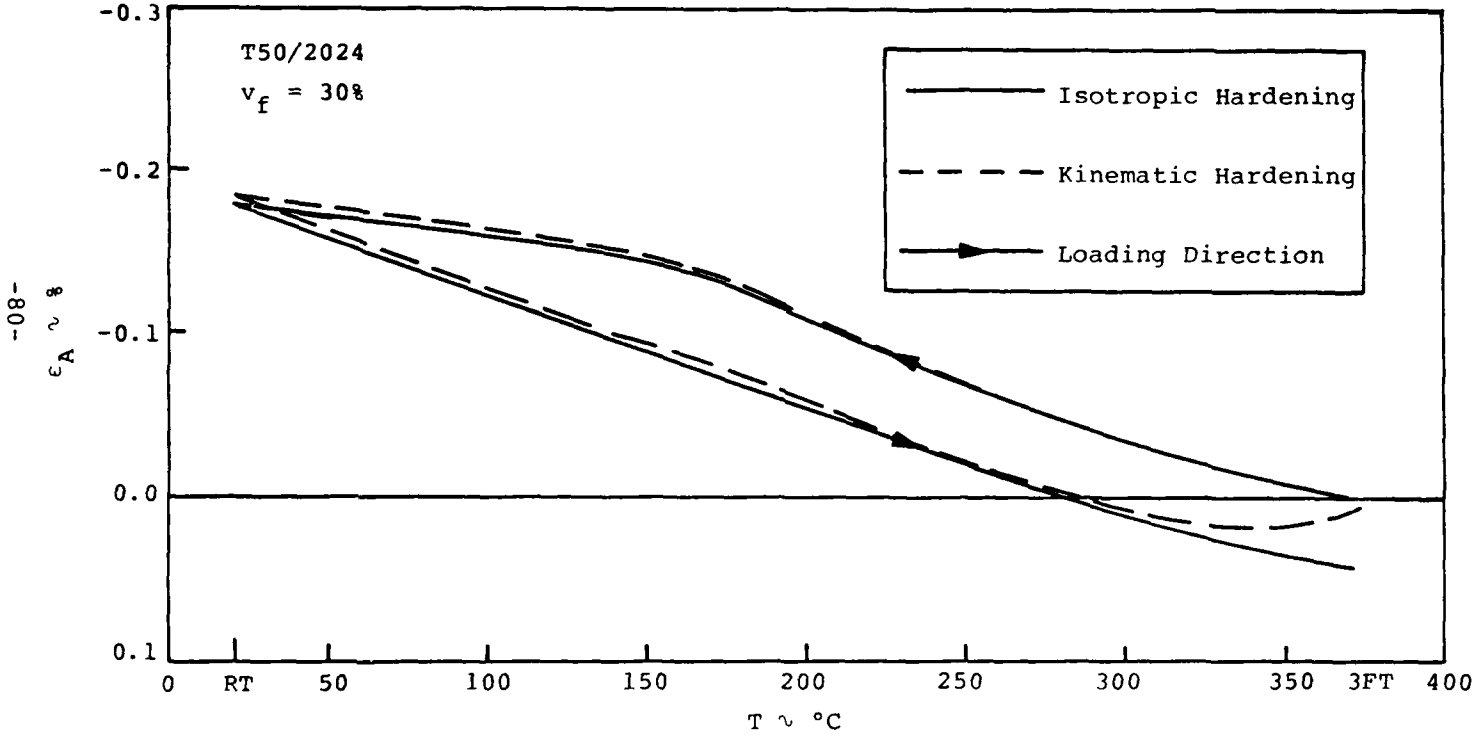

Figure 12. Axial Thermal Expansion, Isotropic vs. Kinematic Hardening

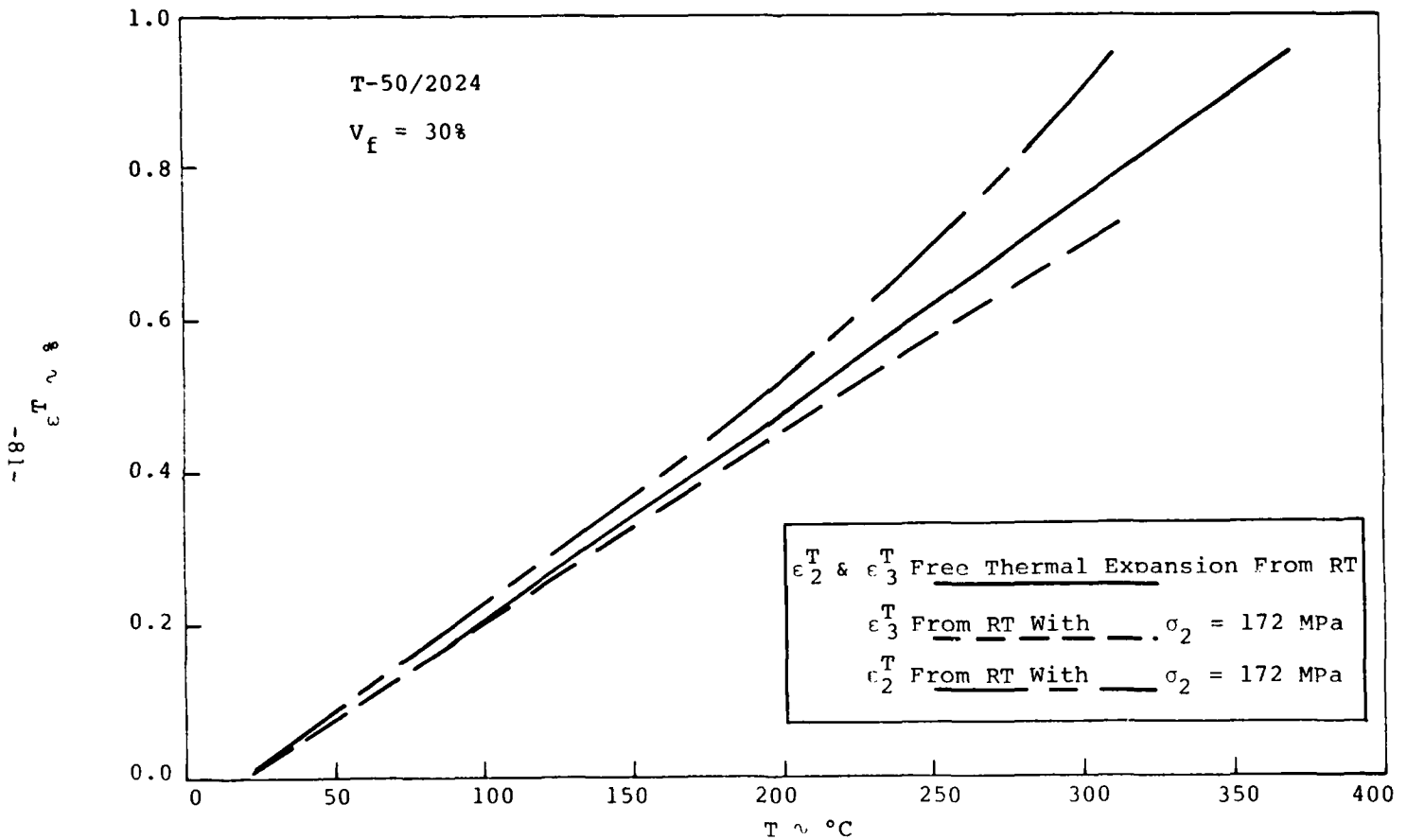

Figure 13. Effect of Applied Stress on Transverse Thermal Expansion, Isotropic Hardening

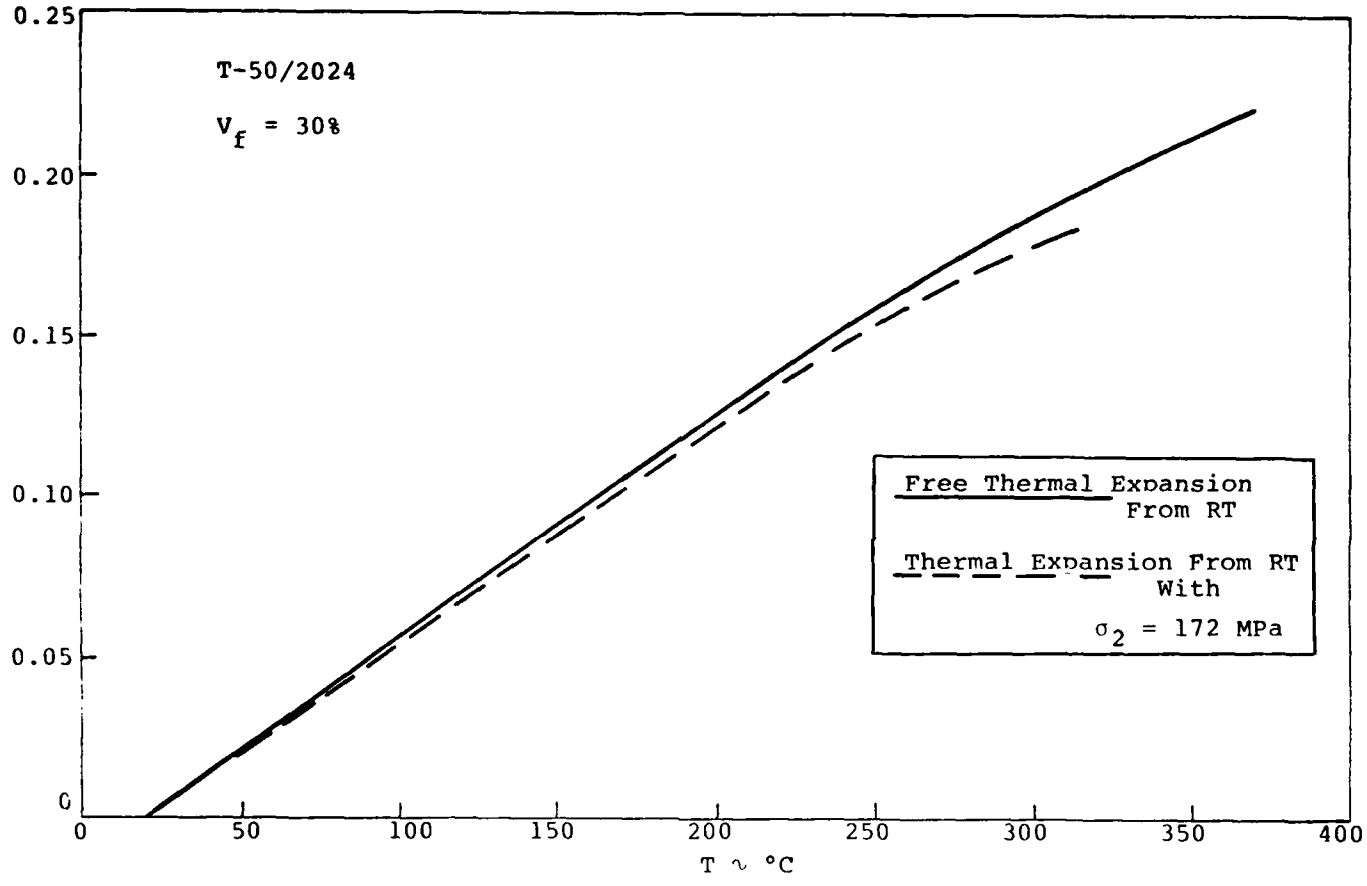

Figure 14. Effect of Applied Stress on Axial Thermal Expansion, Isotropic Hardening

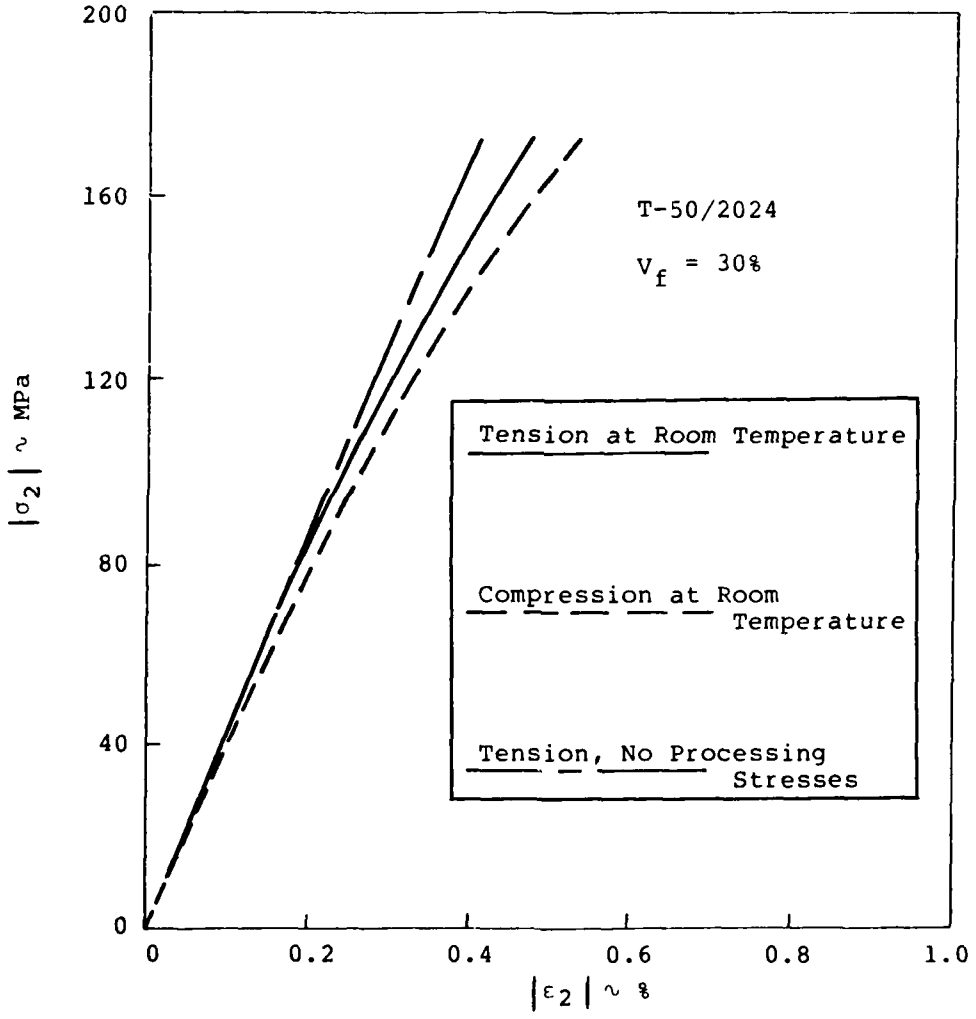

Figure 15. Transverse Stress-Strain Response, Isotropic Hardening

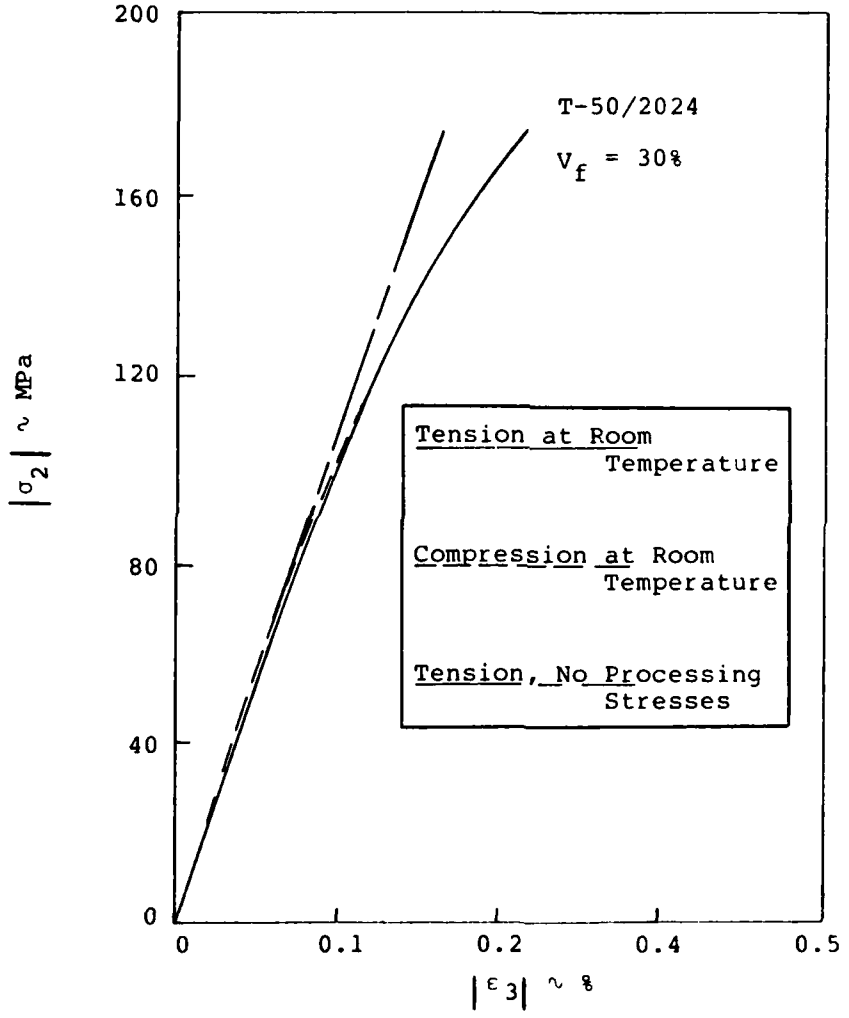

Figure 16. Transverse Normal Strain vs. Transverse Stress, Isotropic Hardening

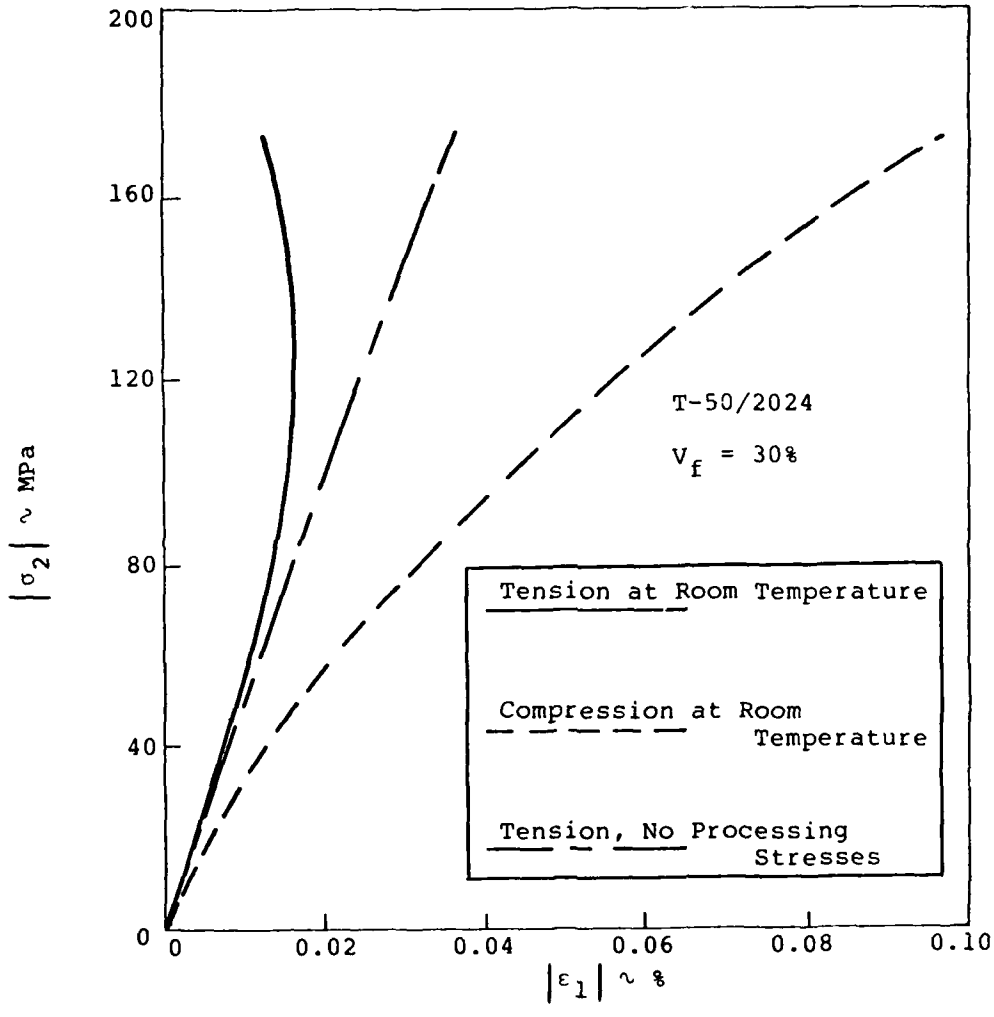

Figure 17. Axial Strain vs. Transverse Stress, Isotropic Hardening

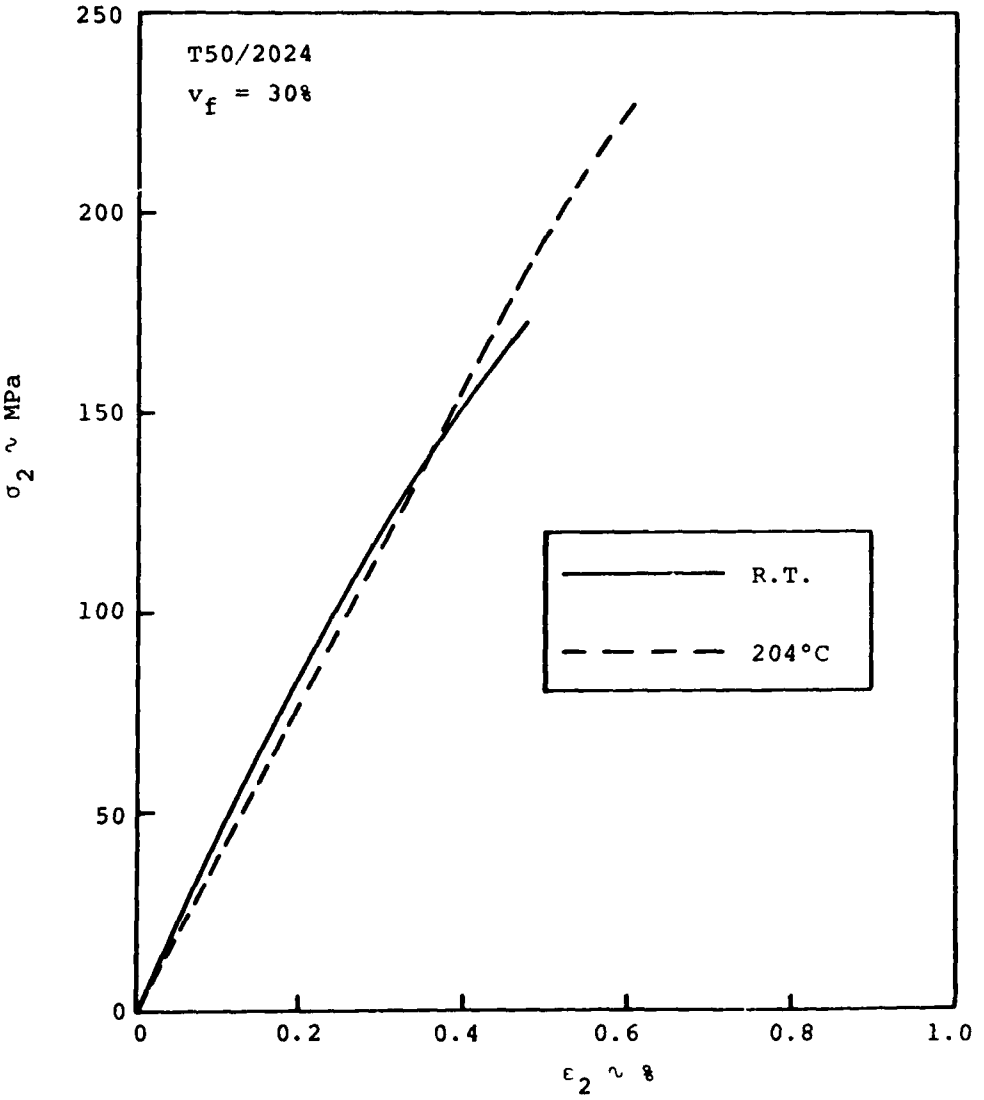

Figure 18. Transverse Tensile Stress-Strain Response at 204°C, Isotropic Hardening

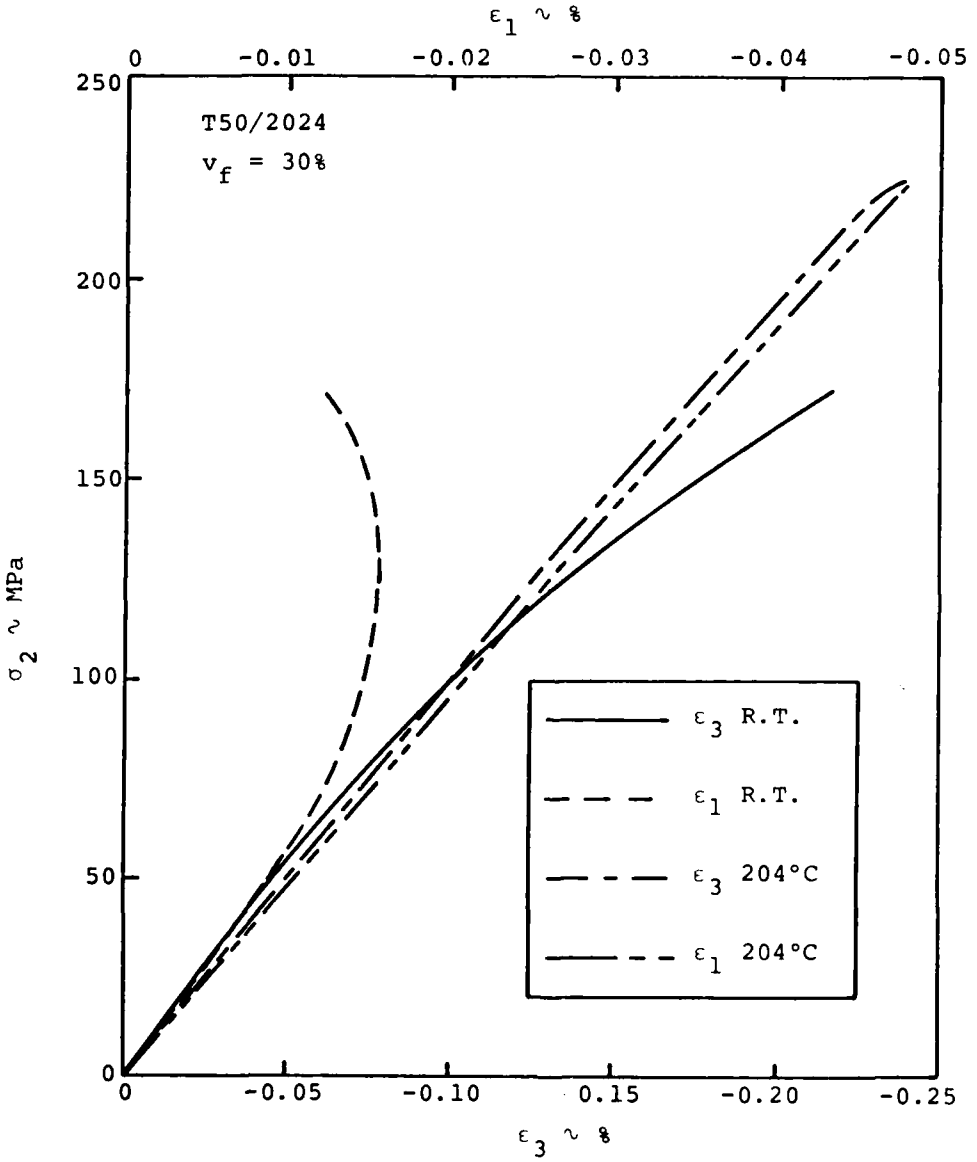

Figure 19. Transverse Normal and Axial Strain vs. Transverse Tensile Stress at 204°C, Isotropic Hardening

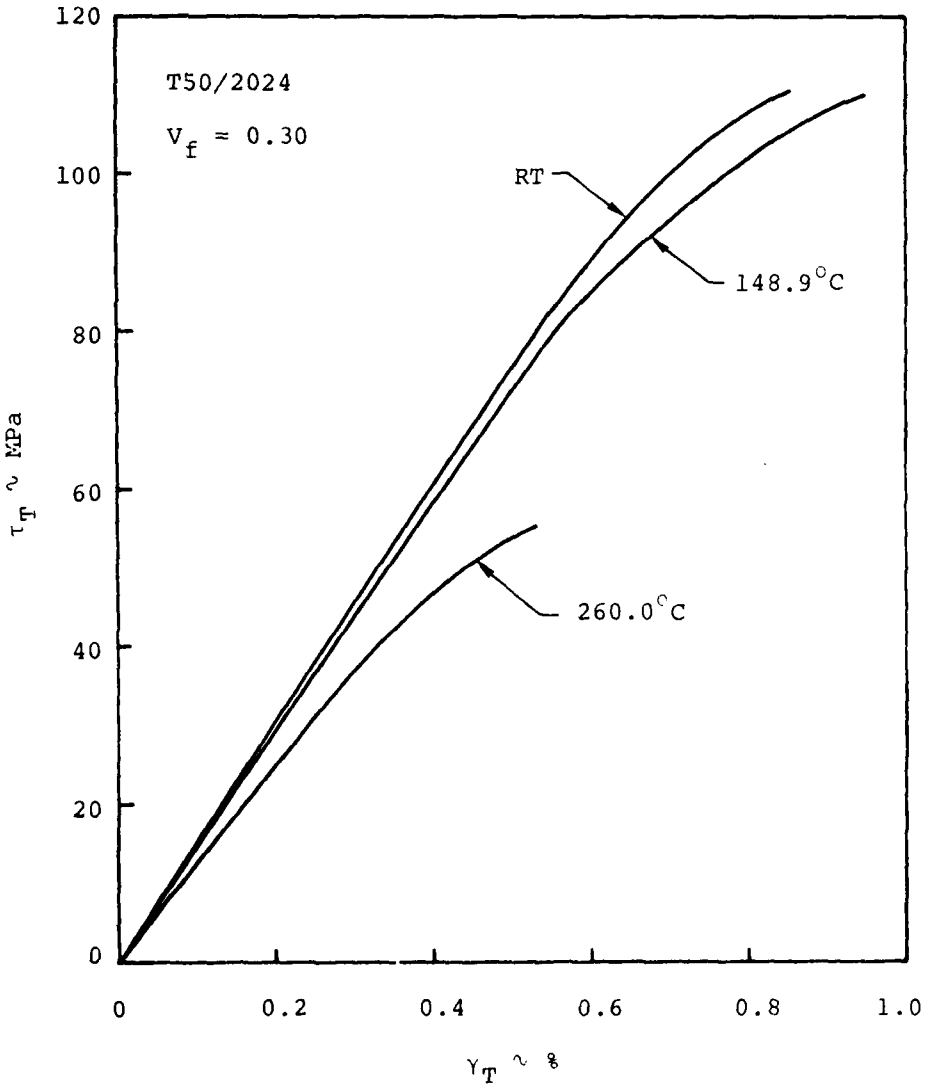

Figure 20. Transverse Shear, No Processing, Isotropic Hardening

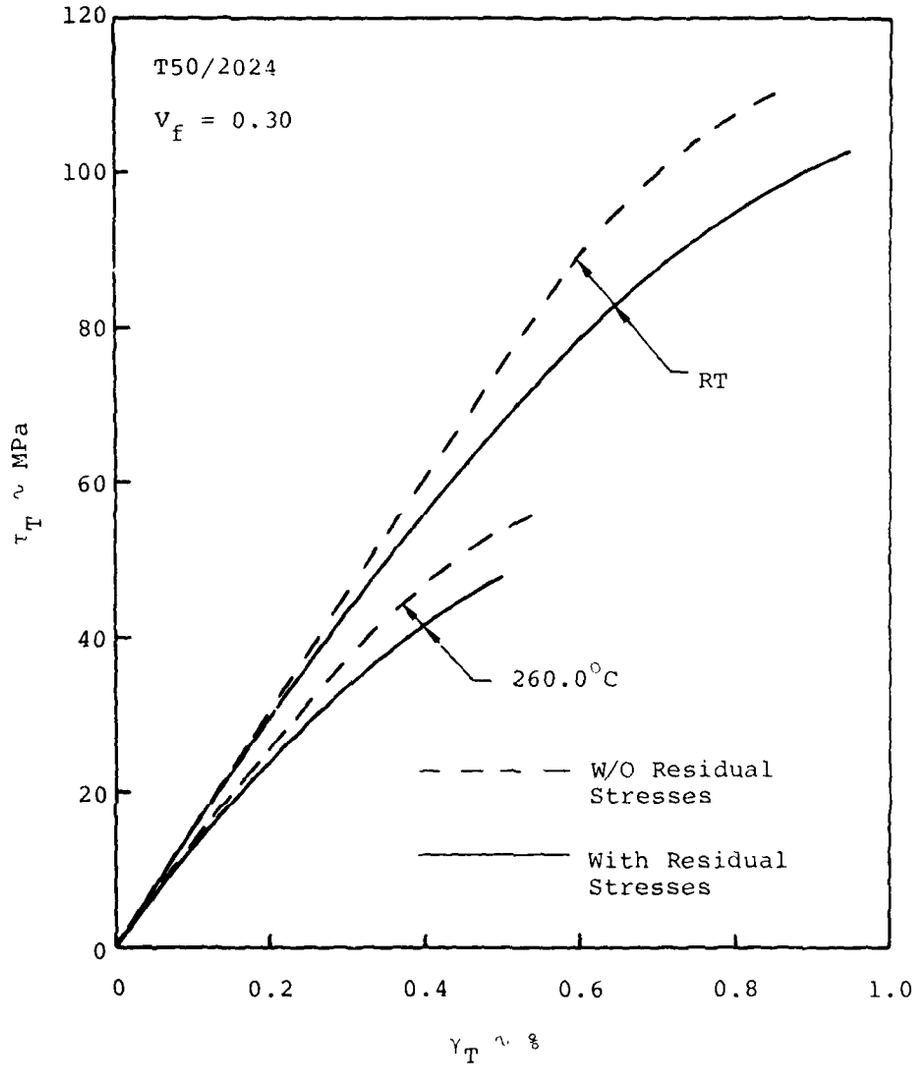

Figure 21. Transverse Shear Stress-Strain Response With and Without Processing, Isotropic Hardening

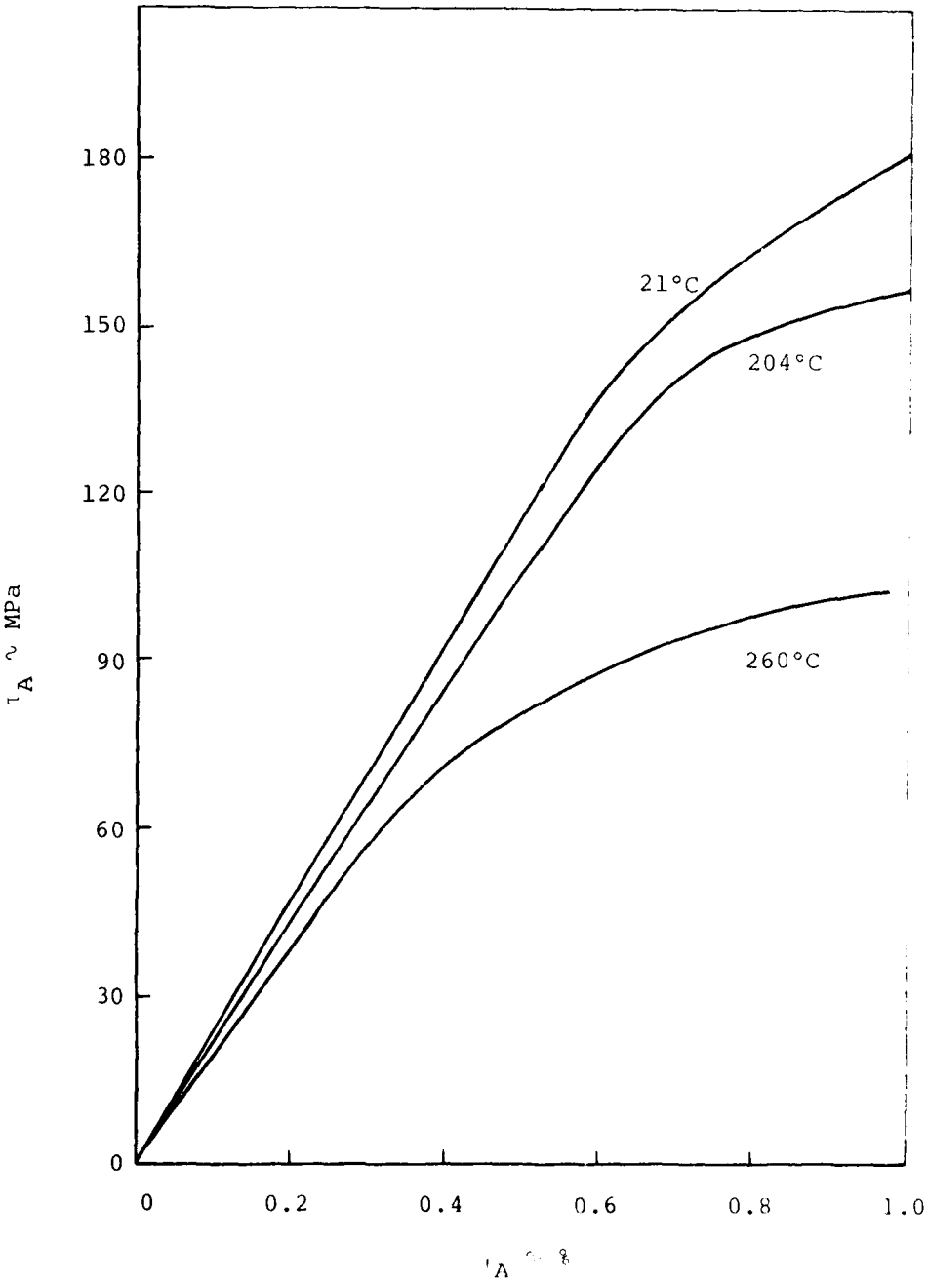

Figure 22. Axial Shear Stress-Strain Response without Processing, Isotropic Hardening

AD-A113 128 MATERIALS SCIENCES CORP SPRING HOUSE PA F/G 11/4
ELEVATED TEMPERATURE BEHAVIOR OF METAL-MATRIX COMPOSITES.(U)
NOV 81 Z HASHIN, E A HUMPHREYS F49620-79-C-0059
UNCLASSIFIED MSC/TFR/1214/1502 AFOSR-TR-82-0212 NL

2 of 2
AD A

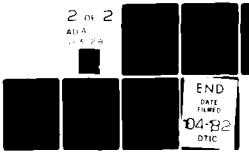

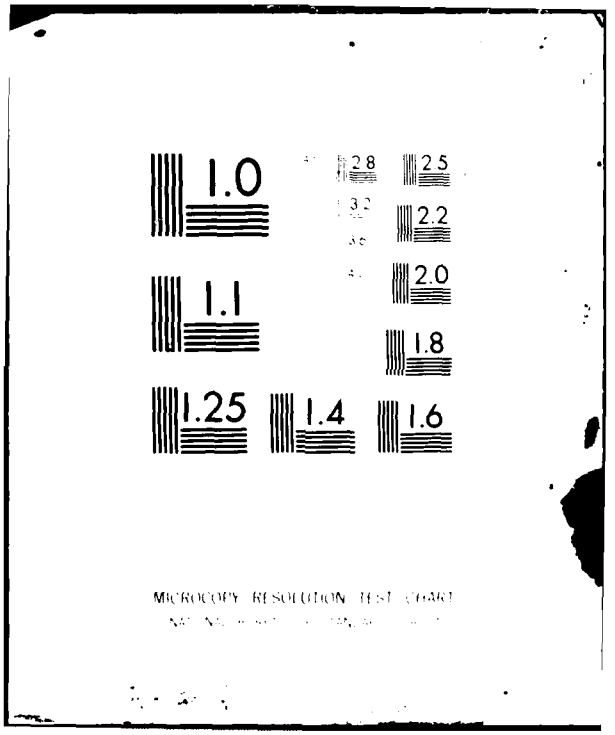
1.0
2.8
2.5
3.2
2.2
2.0
1.1
1.8
1.25
1.4
1.6
MICROCOPY RESOLUTION TEST CHART

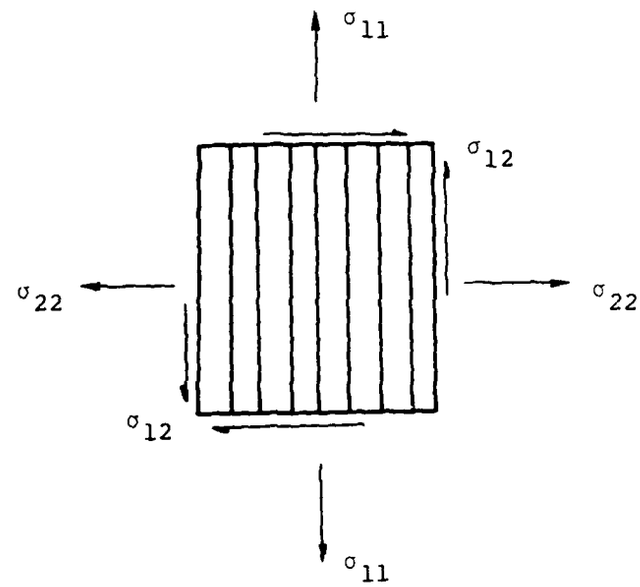

Figure 23. Lamina Plane Stress

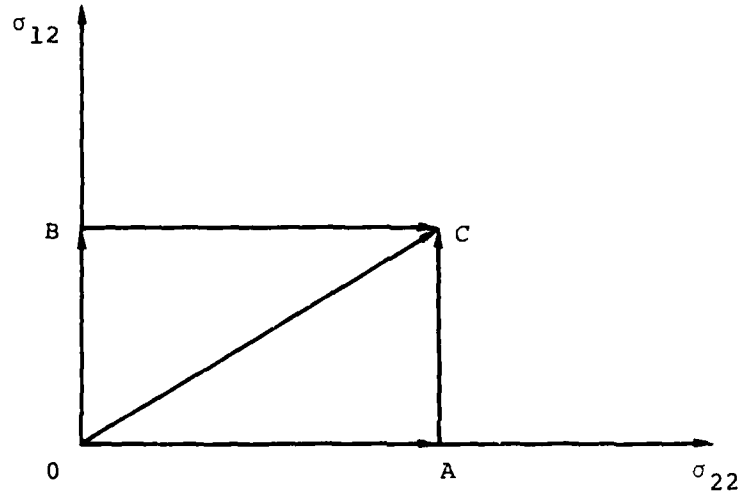

Figure 24. Load Paths

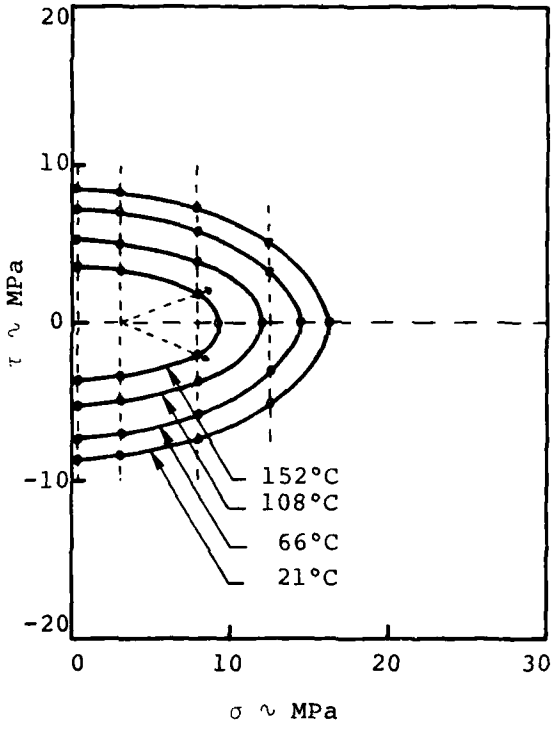

Figure 25. Initial Temperature Dependent Yield Surfaces, Aluminum (Ref. 19)

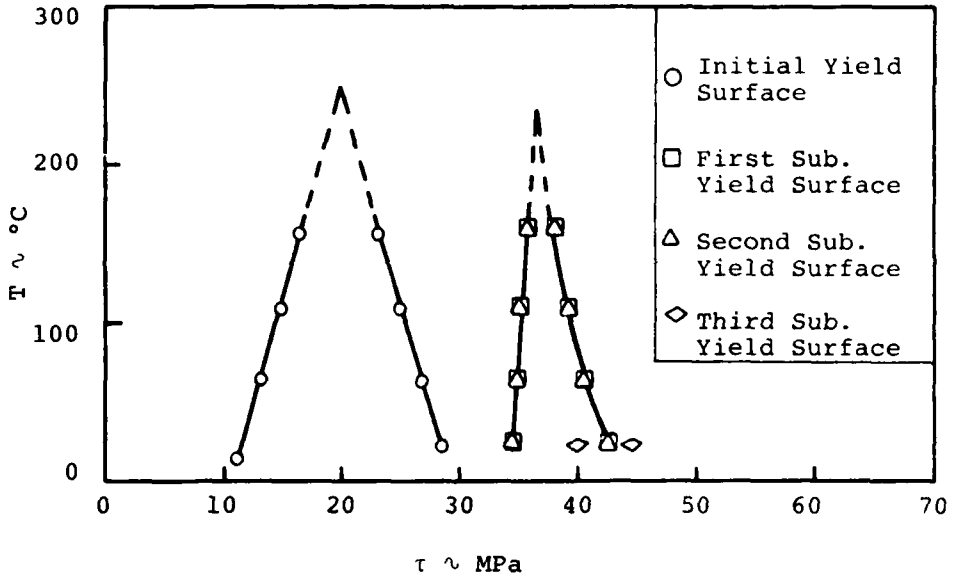

Figure 26. Temperature-Stress Yield Surface Sections, Aluminum, (Ref. 19)

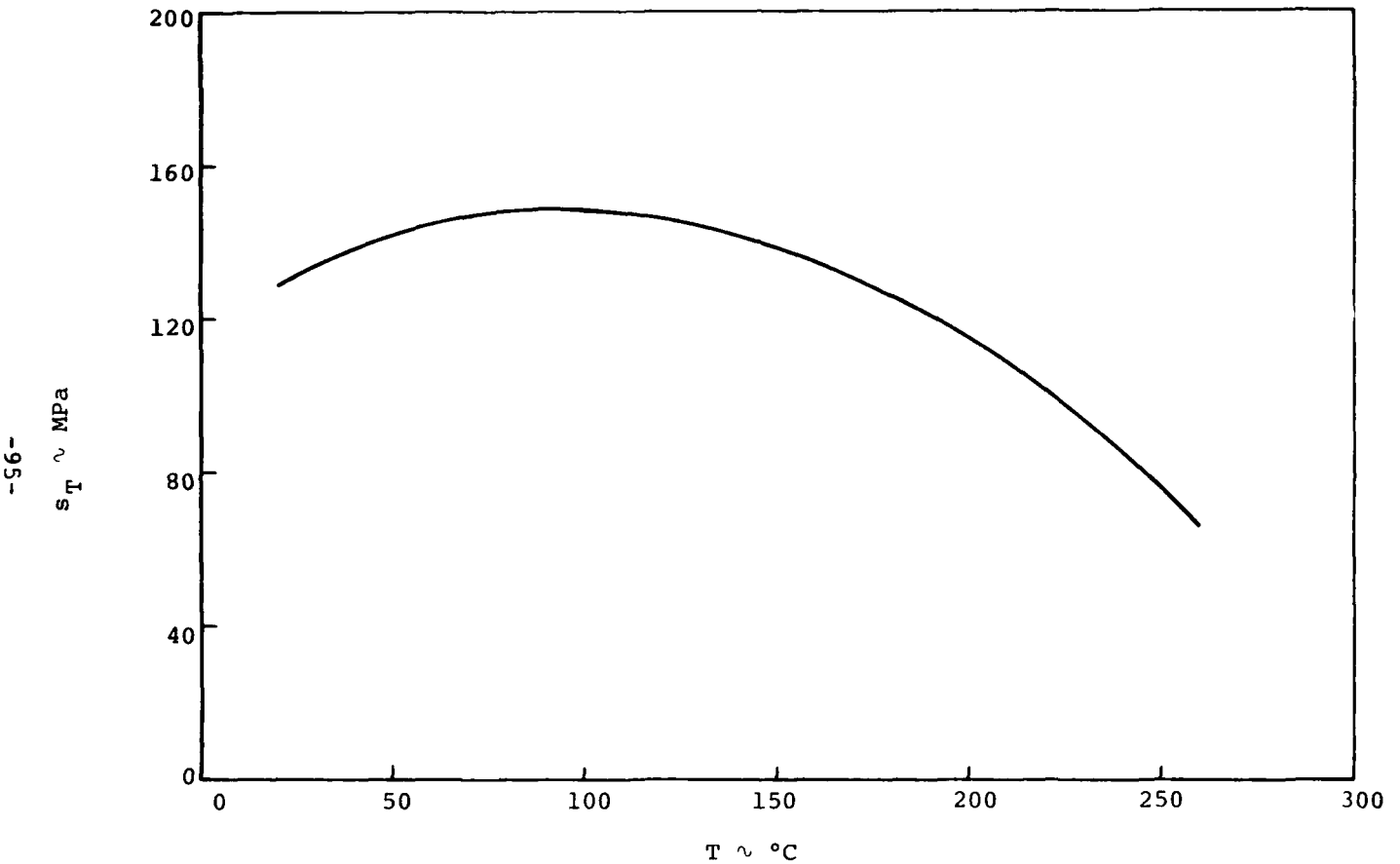

Figure 27. Temperature Dependence of Ramberg-Osgood Parameter s_T

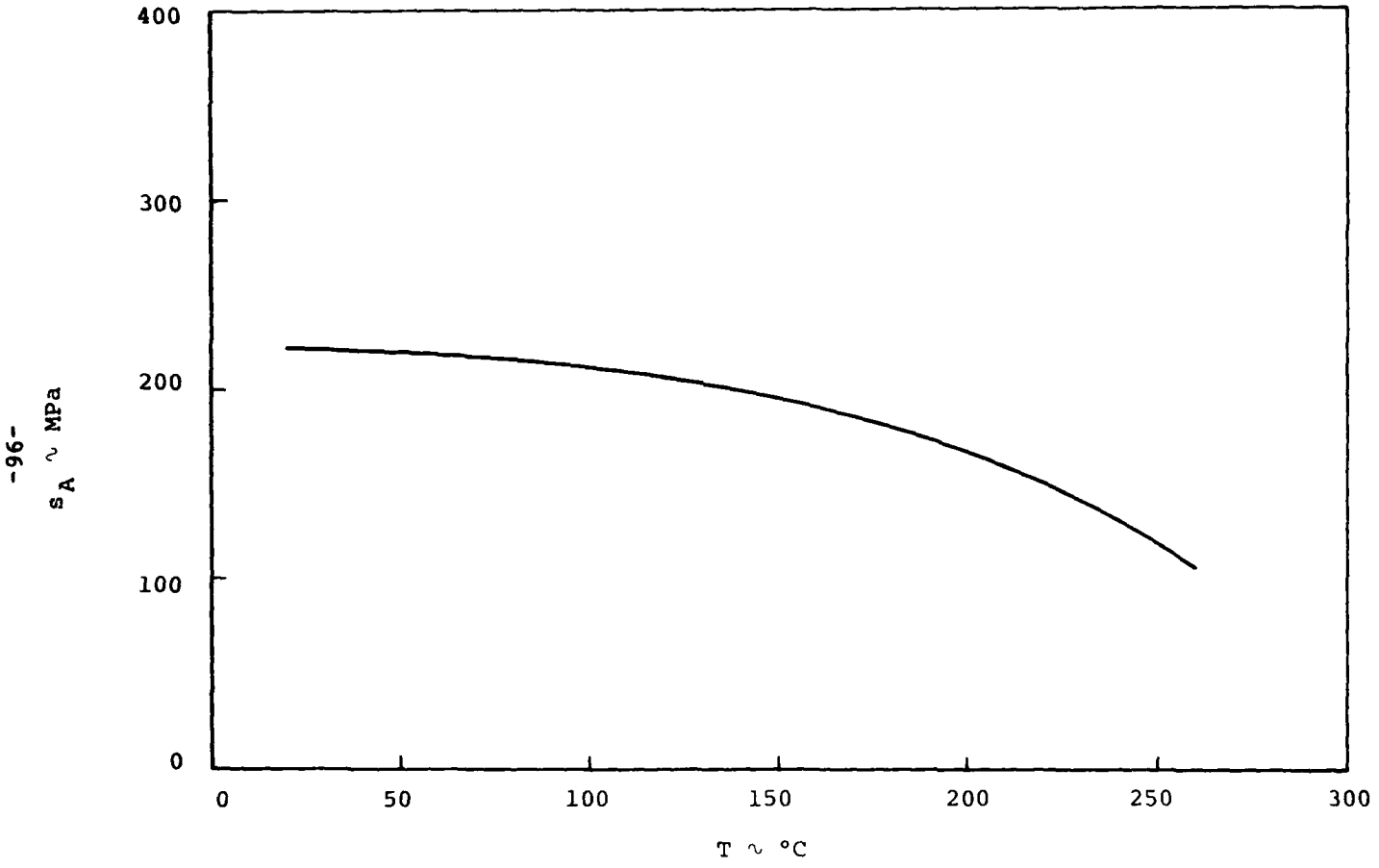

Figure 28. Temperature Dependence of Ramberg-Osgood Parameter s_A

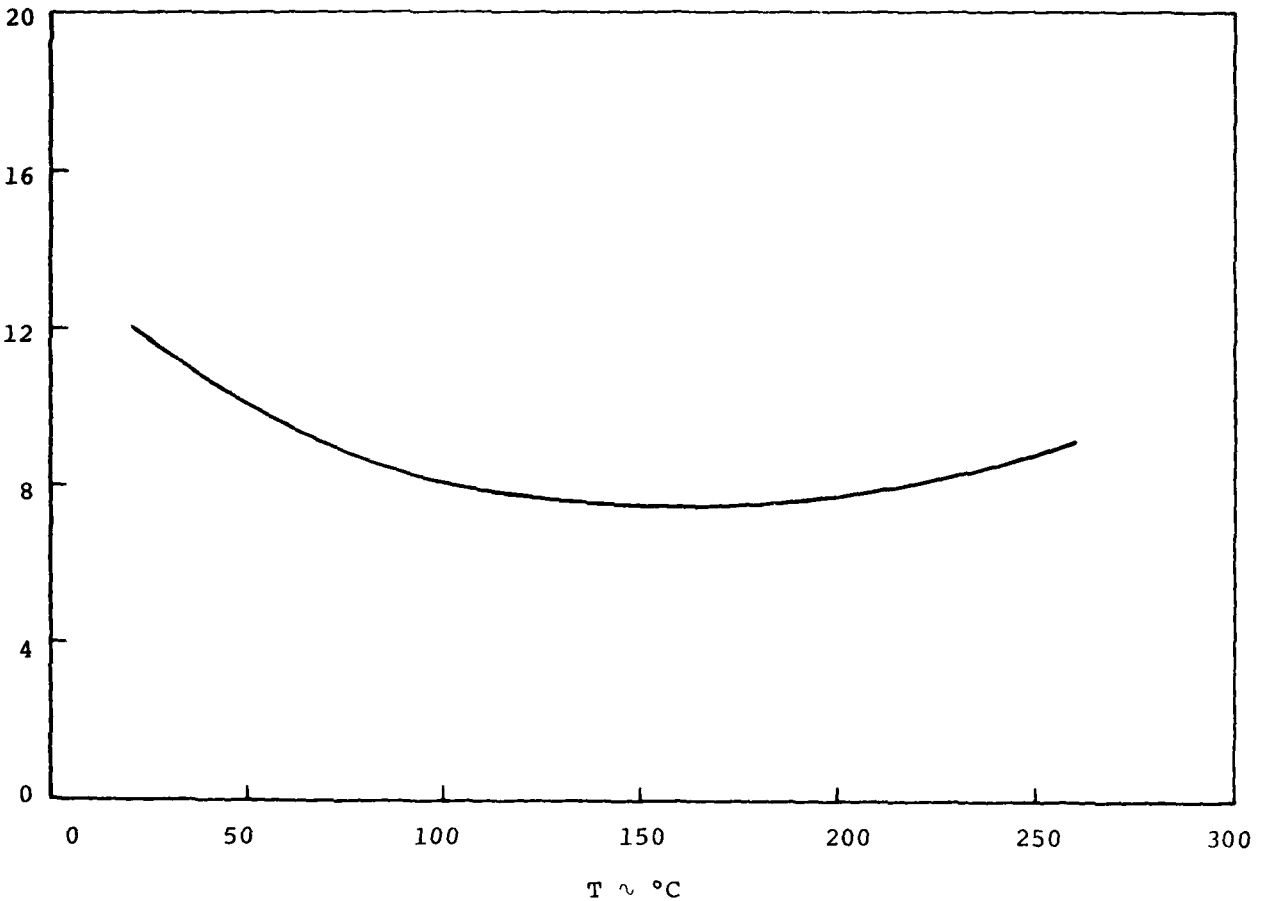

Figure 29. Temperature Dependence of Ramberg-Osgood Parameter m

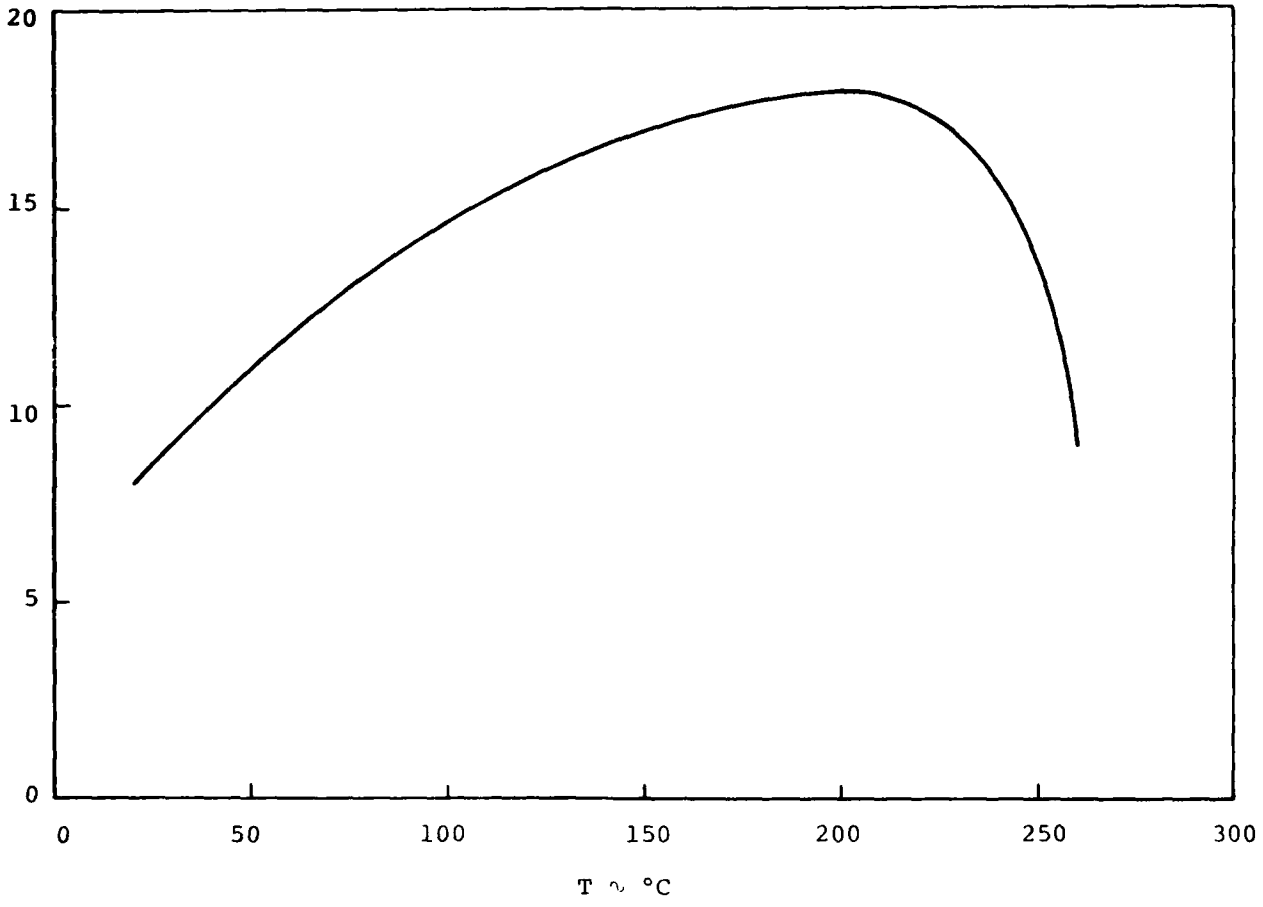

Figure 30. Temperature Dependence of Ramberg-Osgood Parameter n

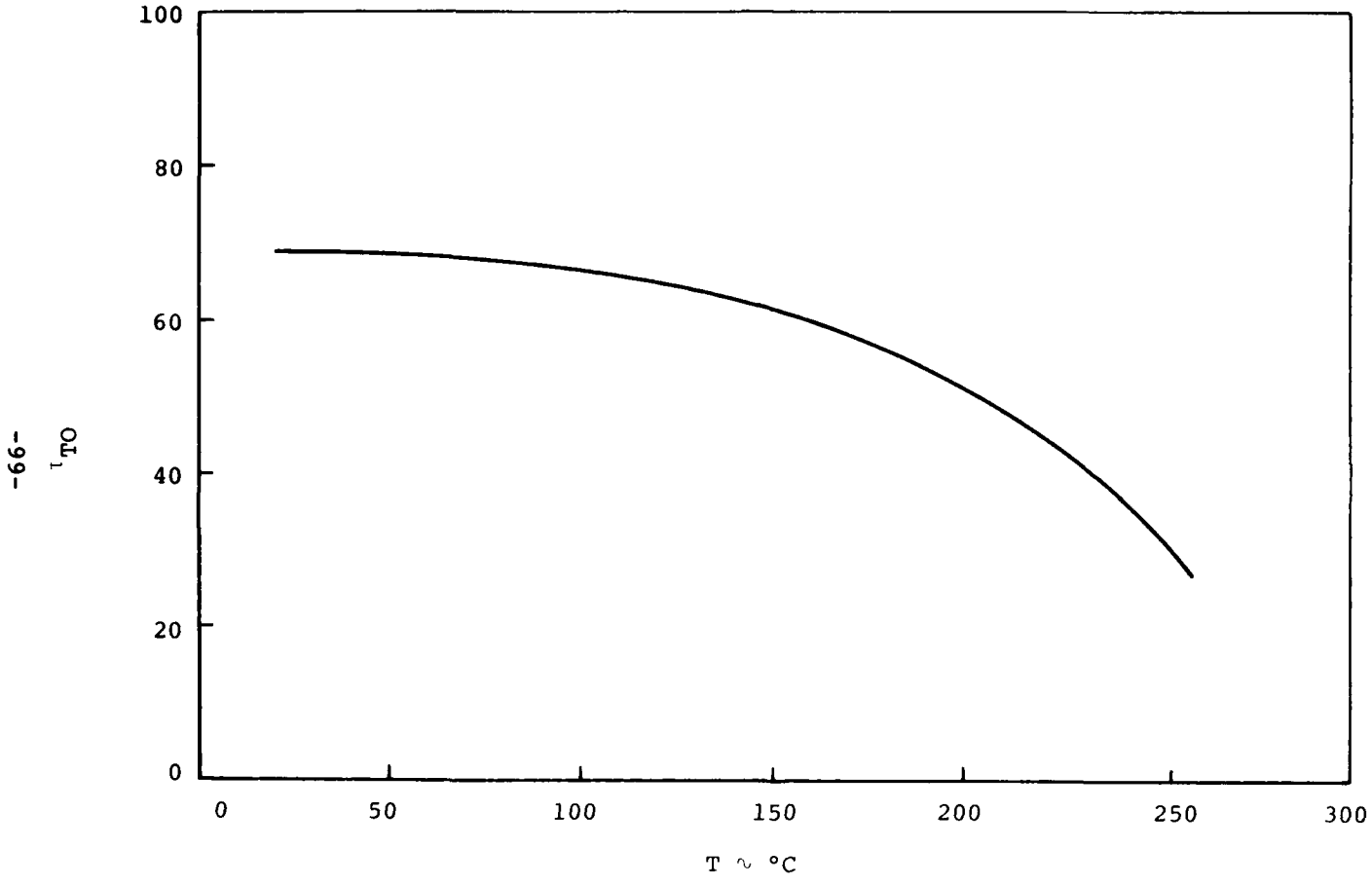

Figure 31. Temperature Dependence of Initial Yield Stress τ_{TO}

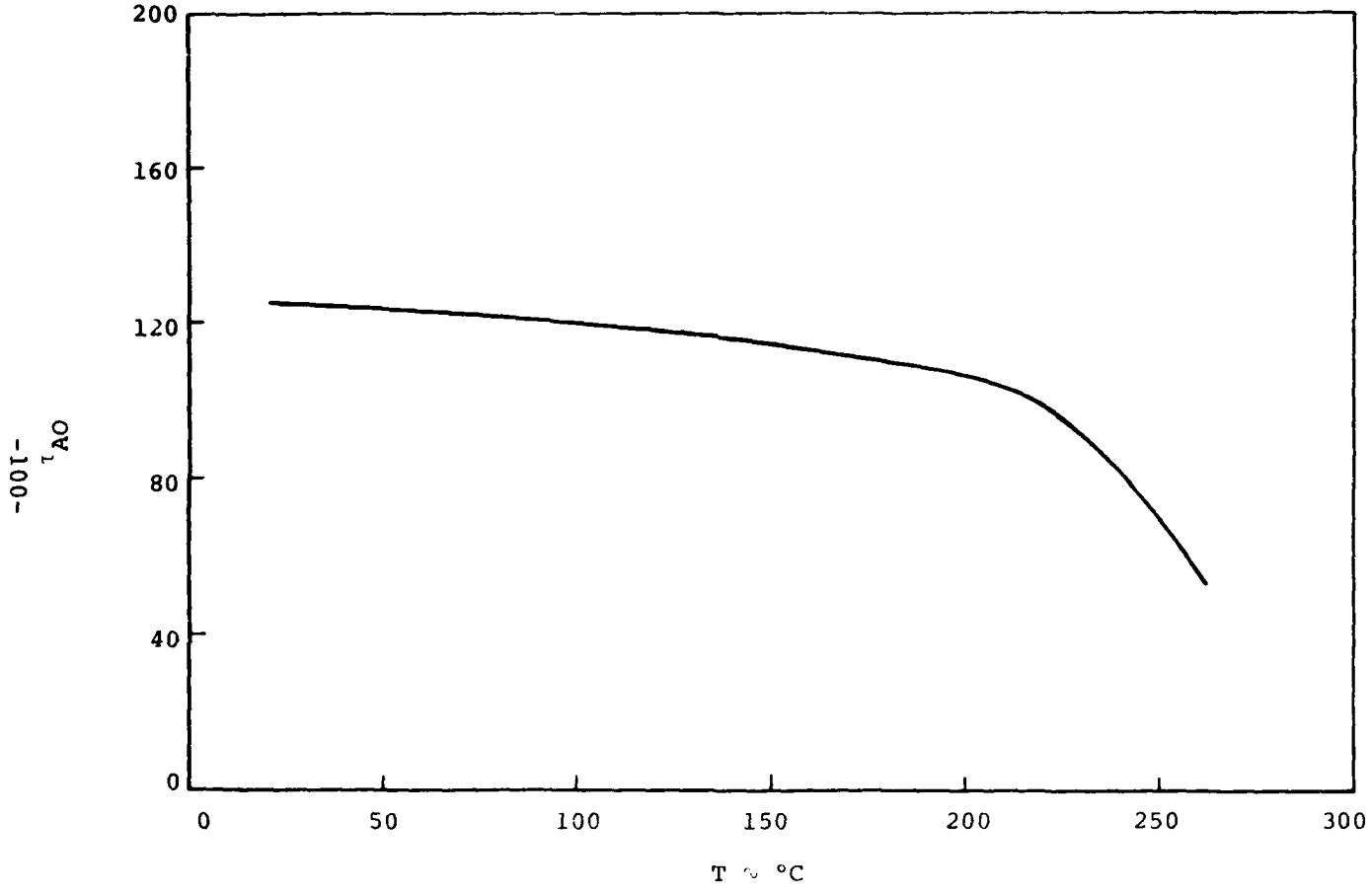

Figure 32. Temperature Dependence of Initial Yield Stress τ_{AO}

APPENDIX A
ANSYS PLASTICITY

The finite element analysis code utilized in the current study was ANSYS. This is a proprietary computer code developed and maintained by Swanson Analysis Systems, Inc. ANSYS is a general multipurpose finite element code with many capabilities.

Two different hardening rules were used in the metal-matrix composite analysis. Both isotropic hardening and classical bilinear kinematic hardening were considered for the aluminum matrix material. The development of these two hardening rules is fundamentally different in ANSYS, even though the yield conditions (von Mises) and flow rules (Prandtl-Reuss) are identical. A brief synopsis of the pertinent elements of the derivations of the two plasticity approaches is given here. A more detailed description can be found in reference 16.

ISOTROPIC HARDENING

In ANSYS, isotropic hardening in two or more dimensions is developed as an extension of a one-dimensional case. The process involves computing equivalent, one-dimensional stresses and strains for evaluating the yield condition. The procedure is as follows.

First, a one-dimensional strain which includes plasticity effects is computed at iteration i.

$$\varepsilon_{e,i} = \frac{1}{\sqrt{2}\,(1+\nu_e)} \left\{ (\varepsilon_x^t - \varepsilon_y^t)^2 + (\varepsilon_y^t - \varepsilon_z^t) + (\varepsilon_z^t - \varepsilon_x^t) + \frac{3}{2}(\gamma_{xy}^t)^2 \right.$$

$$\left. + \frac{3}{2}(\gamma_{yz}^t)^2 + \frac{3}{2}(\gamma_{xz}^t)^2 \right\}^{1/2} \qquad \text{(A-1)}$$

where ε_j^t = total strain-thermal strain-origin shift strain.*

*An artificial strain which accounts for stress reversal, defined later.

This strain is compared to the previous maximum ε_{max} and loading is occurring if $\varepsilon_{e,i} > \varepsilon_{max}$. If this is the case, then ε_{max} is set equal to $\varepsilon_{e,i}$. Based on $\varepsilon_{e,i}$ and the input stress-strain curves, a one-dimensional equivalent stress, $\sigma_{e,i}$, is computed.

In equation A-1, ν_e is defined as:

$$\nu_{e,i} = \frac{1}{2} - (\frac{1}{2} - \nu) \frac{\sigma_{e,i}}{E\ \varepsilon_{e,i}} \tag{A-2}$$

thus, $\sigma_{e,i}$ and $\varepsilon_{e,i}$ are related and the computation must be made iteratively. A quantity $(d\sigma_e/d\varepsilon_p)_{i-1}$ is now computed:

$$(\frac{d\sigma_e}{d\varepsilon_p})_{i-1} = \frac{1}{\frac{\varepsilon_{e,i} - \varepsilon_{e,i-1}}{\sigma_{e,i} - \sigma_{e,i-1}} - \frac{1}{E}} \tag{A-3}$$

which is the rate of change of equivalent stress to plastic strain. Utilizing this, the plastic strain increment can be calculated.

$$\Delta\varepsilon_p = \frac{\varepsilon_{et} - \frac{2}{3}\frac{1+\nu}{E}\sigma_{e,i-1}}{\frac{2}{3}(1-\nu)(1+\frac{1}{E}[\frac{d\sigma_e}{d\varepsilon_p}]_{p,i-1})} \tag{A-4}$$

where

$$\varepsilon_{et} = \frac{\sqrt{2}}{3}\Big\{(\varepsilon_x'-\varepsilon_y')^2 + (\varepsilon_y'-\varepsilon_z')^2 + (\varepsilon_z'-\varepsilon_x')^2 + \frac{3}{2}(\gamma_{xy}')^2 + \frac{3}{2}(\gamma_{yz}')^2 + \frac{3}{2}(\gamma_{xz}')^2\Big\}^{1/2} \tag{A-5}$$

and $\varepsilon_j' = \varepsilon_j^t$ - plastic strain.

With $\Delta\varepsilon_p$, ε_{et}, and ε_j^1 defined, the plastic strain components are computed from the Prandtl-Reuss flow rules.

$$\Delta\varepsilon_x^p = \frac{\Delta\varepsilon_p}{3\varepsilon_{et}} (2\varepsilon_x' - \varepsilon_y' - \varepsilon_z')$$

$$\Delta\varepsilon_y^p = \frac{\Delta\varepsilon_p}{3\varepsilon_{et}} (2\varepsilon_y' - \varepsilon_z' - \varepsilon_x')$$

$$\Delta\varepsilon_z^p = -\Delta\varepsilon_x^p - \Delta\varepsilon_y^p \qquad \text{(A-6)}$$

$$\Delta\gamma_{xy}^p = \frac{\Delta\varepsilon_p}{3\varepsilon_{et}} \gamma_{xy}'$$

$$\Delta\gamma_{yz}^p = \frac{\Delta\varepsilon_p}{3\varepsilon_{et}} \gamma_{yz}'$$

$$\Delta\gamma_{xz}^p = \frac{\Delta\varepsilon_p}{3\varepsilon_{et}} \gamma_{xz}'$$

If unloading is occurring, based on ε_{max} comparisons, then another equivalent, elastic, strain is computed.

$$\varepsilon_s = \frac{1}{\sqrt{2}(1+\nu)} \left\{ (\varepsilon_x^e - \varepsilon_y^e)^2 + (\varepsilon_y^e - \varepsilon_z^e)^2 + (\varepsilon_z^e - \varepsilon_x^e)^2 \right.$$

$$\left. + \frac{3}{2}(\gamma_{xy}^e)^2 + \frac{3}{2}(\gamma_{xz}^e)^2 + \frac{3}{2}(\gamma_{yz}^e)^2 \right\}^{1/2} \qquad \text{(A-7)}$$

where ε_i^e are elastic strains.

The equivalent stress during unloading is simply:

$$\sigma_{e,i} = E\, \varepsilon_s \,. \qquad \text{(A-8)}$$

If $\epsilon_{max} < 0$, the unloading logic is complete. The conditions required for the negative ϵ_{max} are described later.

Since the equivalent stresses and strains used in the derivation are all positive, special provisions are made for evaluating load reversal during the unloading process. Specifically, the largest elastic normal strain component is compared to its corresponding plastic strain component. If they have opposite signs then the material is assumed to be unloading. To account for this, certain corrections to the strains are made. These include:

$$\epsilon_{max} = - |\epsilon_{max}|$$

Current origin shift strains = previous origin shift strains + 2 previous plastic strains

Current plastic strains = -previous plastic strains

$$\epsilon_{e,i} = \epsilon_{s,i} \qquad (A\text{-}9)$$

The effects of these adjustments is to convert the unloading into loading by shifting the origin and reversing the sign of the plastic strains. As was stated previously, the isotropic hardening used is an extension of one-dimensional plasticity. This manifests itself in the stress reversal evaluation and therefore the isotropic hardening is not recommended for general three-dimensional plasticity. The analyses made under the isotropic hardening rules have been shown to be consistent within themselves and with the kinematic hardening analyses, however.

KINEMATIC HARDENING

The classical bi-linear kinematic hardening used in ANSYS does not suffer the reversed loading difficulties found in the isotropic hardening behavior analysis. This is because it is

not developed as an extension of a one-dimensional case.

For the kinematic hardening, the plastic strain increment is defined differently. Specifically, the ε_{et} (eqn. A-5) term is defined in terms of $\varepsilon_j' - \varepsilon_j^{sh}$ instead of ε_j' and the yield stress is used instead of $\sigma_{e,i}$. The strain ε_j^{sh} is defined such that $E\varepsilon_j^{sh}$ equals the increase in stress above the yield stress. In addition, the term $(d\sigma_e/d\varepsilon_p)_{i-1}$ is defined as $E(S)/1-S$, where $(S)E$ is the slope of the second line on part of the input bi-linear stress-strain curves. When the computed value of $\Delta\varepsilon_p$ (eqn. C-4) is greater than zero, yielding is occurring. Otherwise, unloading is occurring. A specific example given in reference 16 for the various strain calculations is:

$$(\varepsilon_x^e)_i = (\varepsilon_x')_i - \Delta\varepsilon_x^p$$

$$(\varepsilon_x^{pl})_i = (\varepsilon_x^{pl})_{i-1} + \Delta\varepsilon_x^p \qquad \text{(A-10)}$$

$$(\varepsilon_x^{sh})_i = (\varepsilon_x^{sh})_{i-1} + \Delta\varepsilon_x^p \frac{2(1+\nu)}{2} \frac{S}{1-S}$$

The term $E\varepsilon_j^{sh}$ is the amount that the yield surface is shifted within the stress space, in the j-direction. Since the relations do not use the equivalent stresses or strains for evaluating the plasticity effects, reversed loading behavior is handled directly and adjustments required for isotropic hardening are not needed.

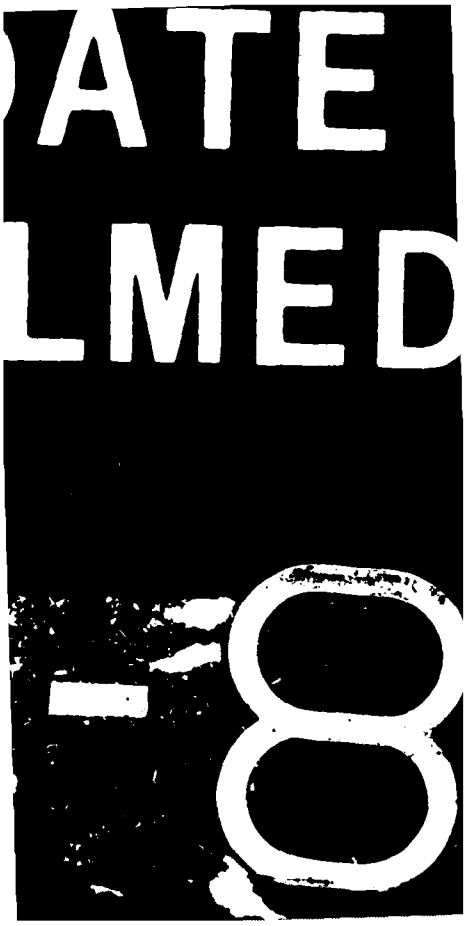
ATE
LMED
8